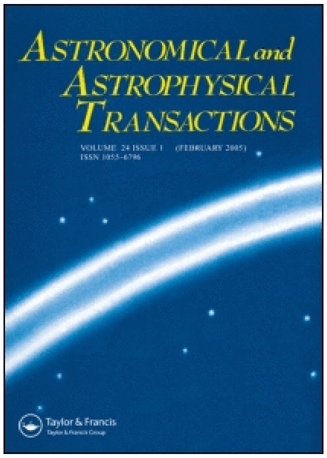

Astronomical & Astrophysical Transactions
The Journal of the Eurasian Astronomical Society
Publication details, including instructions for authors and subscription information:
http://www.informaworld.com/smpp/title~content=t713453505

Spectrophotometry of 83 possible blue compact dwarf galaxies from the second byurakan survey

Yu. I. Izotov [a]; V. A. Lipovetsky [b]; N. G. Guseva [a]; A. Yu. Kniazev [b]; S. I. Neizvestny [b]; J. A. Stepanian [b]
[a] Main Astronomical Observatory, Ukrainian AS, Kiev, Ukraine
[b] Special Astrophysical Observatory, Russian AS, Stavropol region, Russia

Astronomical and Astrophysical Transactions, 1993, Vol. 3, pp. 197–236
Reprints available directly from the publisher.
Photocopying permitted by license only

SPECTROPHOTOMETRY OF 83 POSSIBLE BLUE COMPACT DWARF GALAXIES FROM THE SECOND BYURAKAN SURVEY

YU. I. IZOTOV,*[1] V. A. LIPOVETSKY,[2] N. G. GUSEVA,[1]
A. YU. KNIAZEV,[2] S. I. NEIZVESTNY[2] and J. A. STEPANIAN[2]

[1]*Main Astronomical Observatory, Ukrainian AS, Goloseevo, SU-252127 Kiev, Ukraine.*
[2]*Special Astrophysical Observatory, Russian AS, SU-357140 Nyzhny Arhyz, Stavropol region, Russia*

(16 August, 1992)

Spectrophotometric observations of 83 possible blue compact dwarf galaxies (BCDGs) and photoelectric UBVR (Johnson system) observations of 37 galaxies from this list are discussed. The observations have been made with the 6-meter telescope of Special Astrophysical Observatory of Russian Academy of Sciences. The general characteristics of BCDGs are considered. Most galaxies are shown to have very low heavy element abundance.

KEY WORDS Blue compact dwarf galaxies, spectrophotometry, chemical composition.

1. INTRODUCTION

The studies of the blue compact dwarf galaxies (BCDGs) which were carried out during about last 20 years have revealed some interesting properties. These properties are of prime importance for solution of the problems of galaxy formation, chemical evolution, and evolution of luminous stars with the chemical composition different from the solar one. Some important feature of the BCDGs are:

1. Star formation in the BCDGs occurs in starbursts with duration of $\sim 10^7$ years (Searle and Sargent, 1972). During such period, a galaxy has one or several giant, highly excited HII regions.

2. The gas in the regions of ionized hydrogen is deficient of heavy elements. The observed range of heavy element mass fraction Z varies from 1/70 to 1/2 of the solar value (Kunth and Sargent, 1983, Campbell *et al.*, 1986, Skillman *et al.*, 1988, Izotov *et al.*, 1990). Thus, the BCDGs are relatively unevolved stellar systems which have not as yet progressed in the enrichment of their gas with the products of earlier evolution of stars as far as giant galaxies have done. It is the study of the physical conditions in the BCDG HII regions based on spectral

* Author to whom correspondence should be addressed.

observations which allows to determine the primeval abundance of helium and to shed light on early galactic evolution.

3. In some blue compact dwarf galaxies, the old stellar population has not been observed (Kunth *et al.*, 1988). This implies that these galaxies may be really young, i.e., they undergo the first burst of star formation.

The properties of the BCDGs mentioned above encourage their search in deep surveys. The main criteria of the BCDG selection were as follows:

1. The BCDGs are compact objects with ultraviolet excesses. The samples of the blue compact dwarf galaxies selected basing on photometric and morphological properties are given in Takase (1980), Zwicky (1966) and Bingelli *et al.* (1985).

2. BCDGs have strong emission lines in low-dispersion spectra obtained with Schmidt telescopes with using an objective prism (Smith *et al.*, 1976, Bohuski *et al.*, 1978, Kunth *et al.*, 1981, Salzer *et al.*, 1989, Markarian *et al.*, 1989).

The second criterion of the BCDG selection is somewhat better for subsequent determination of the galaxy chemical composition because of the selection of galaxies with strong emission lines.

The Second Byurakan Survey (SBS) is probably one of the deepest spectral survey containing a large number of blue compact dwarf galaxies. In 1988 we started the program of spectral and photometric observations of blue compact dwarf galaxies with highly excited HII regions. Our main purposes were as follows:

—search of the galaxies with extremely low abundance of heavy elements. These are the galaxies which might be really young;

—determination of the content of the primeval helium;

—study of stellar population in the regions of ionized hydrogen;

—solution of the problems of chemical evolution in BCDGs;

—study of the large-scale distribution of BCDGs.

The candidates for observations were chosen on the basis of low-dispersion spectra of the Second Byurakan Survey. These spectra were obtained on the 1-m Schmidt telescope with an objective prism in Byurakan Observatory of the Armenian Academy of Sciences (Markarian *et al.*, 1983). The Second Byurakan Survey covers the region of sky with right ascensions $\alpha = 7^h–17^h$, and declinations $\delta = +49°–+61°$ and some other additional areas on the sky.

The large intensities of emission lines and weak continuum were the main criteria for our selection of possible BCDG galaxies with HII regions of high excitation. Observations of some Markarian galaxies from the First Byurakan Survey (FBS) were carried out together with the galaxies from the Second Byurakan Survey. The total list contains about 400 galaxies. In the present paper the results of spectral observations of 83 galaxies and the photometric observations of 37 galaxies from the list of the candidates for blue compact dwarf galaxies are given.

2. OBSERVATIONS AND DATA REDUCTION

Spectral and photometric observations of the galaxies were carried out during Sept. 1988–Apr. 1990, on the 6-m telescope of the Special Astrophysical Observatory of the USSR Academy of Sciences (SAO AS USSR) with the use of the 1024-channel photon counter: the scanner. The journal of observations is given in Table 1 which contains the galaxy name; the right ascension α and declination δ of the galaxies for the 1950.0 epoch; the visual estimate of the photographic apparent magnitude m_v, given by authors of SBS from plates obtained with 1-m Schmidt telescope at the Byurakan Observatory; exposure in sec; spectral resolution in Å/channel; the observed redshift z obtained from the wavelengths of bright emission lines. Data processing has been made with the SAO AS USSR standard method of scanner data reduction (Afanasiev *et al.*, 1991). To eliminate the difference in the sensitivity of the object and sky receivers, for the bulk of observed galaxies two exposures close in duration have been made—the first, with the object receiver and the second, with the sky receiver. After processing, these two spectra were combined.

Figure 1 shows spectra of the galaxies obtained with a diffraction grating of spectral resolution 1.9 Å/channel and 3.8 Å/channel.

Photometric observations were carried out on the 6-m telescope with the Nasmyth electrophotometer (Vikuliev *et al.*, 1991). Table 2 presents the results of the photometric observations: the galaxy name is given in column 2; in column 3 the diameter of the diaphragm is given in arcsec; in column 4, the apparent magnitude; the colors (U–B), (B–V) and (V–R) are given in columns 5–7, respectively. The standard differential method of photometric observations has been used. As usual, two measurements of each galaxy in the UBVR Johnson system were made during spectral observations. The observation mode is used when 6% of the object light goes through the photometer channel and 94% of the light goes to the scanner. Before and after the galaxy observations a photoelectric standard located not far from the galaxy, is recorded. The northern sky UBVR standards (Neizvestny, 1987) have been used as the photoelectric standards. Reduction into the standard system and removal of the atmosphere has been carried out according to Neizvestny (1983).

3. CHEMICAL ABUNDANCES IN GALAXIES

The gas abundance in HII regions has been determined from intensities of emission lines observed in the spectra. The data have been corrected for interstellar extinction (Whitford, 1958, Lequex *et al.*, 1979) and for underlying stellar absorption lines of the Balmer series (McCall *et al.*, 1985). The equivalent widths of the hydrogen absorption lines has been taken as 1.9 Å. Table 3 gives: the unshifted wavelengths of the lines, λ_0; corrected emission line intensities: extinction coefficient c (H_β); equivalent width EW (H_β) for the H_β line; the distance to the galaxy d in Mpc; absolute magnitude M_B in the B band and the H_β-luminosity L (H_β) in erg · s^{-1}. The errors of the line intensities given in Table 3 have been derived from the statistics of the signals accumulated in the scanner channels. The adopted value of the Hubble constant is $H_0 = 50$ km · s^{-1} · Mpc^{-1}.

Table 1 Journal of observations

No.	Galaxy SBS	Coordinates, 1950 α	δ	m	Exposure, sec	Resolution	z
1	2	3	4	5	6	7	8
1.	0127+307A	$01^h27^m.9$	$+30°45'.2$	$17^m.0$	1209	2	0.0171
2.	0134+318	01 34.6	+31 52.3	18.0	1203	2	0.0446
3.	0142+046	01 42.1	+04 39.6	18.0	1575	2	0.0056
4.	Mkn 1169	01 55.1	+02 10.8	17.0	640+ 654	2	0.0165
5.	0158+336	01 58.0	+33 39.1	17.0	817	2	0.0378
6.	0335-052	03 35.2	-05 11.7	18.0	846	2	0.0137
7.	0335-057A	03 35.7	-05 41.4	17.5	1717	2	0.0225
8.	0335-057B	03 35.7	-05 44.8	17.5	751	2	0.0911
9.	0745+587	07 45.4	+58 47.2	18.0	1112	2	0.0212
10.	0749+568	07 49.7	+56 48.8	18.0	1161+1077	2	0.0182
11.	0751+570	07 51.8	+56 57.8	18.0	889	2	0.0269
12.	0756+611	07 56.5	+61 07.6	17.5	1294	2	0.0206
13.	0805+607	08 05.2	+60 45.7	17.0	746	2	0.0314
14.	0807+580B	08 08.1	+58 03.5	17.5	1003	2	0.0265
15.	0813+522	08 13.9	+52 11.7	17.0	1162+1172	2	0.0241
16.	0907+543	09 07.6	+54 22.5	17.0	699+1065	2	0.0274
17.	Mkn 1415	09 10.5	+52 26.4	15.5	1188+1203	2	0.0472
18.	0915+556	09 15.7	+55 40.9	17.5	758+ 796	2	0.0491
19.	Mkn 1416	09 17.4	+52 46.9	17.0	1083+1032	2	0.0077
20.	0926+606A	09 26.4	+60 39.7	17.5:	921+1300	2	0.0137
21.	0926+606B	09 26.4	+60 39.9	17.5:	518+ 582	2	0.0133
22.	0926+607	09 26.4	+60 41.6	18.0	742+ 742	2	0.0140

Table 1—(*continued*)

1	2	3	4	5	6	7	8
23.	0940+544	09 40.9	+54 25.2	18.0	1527+1527	2	0.0057
24.	0943+561A	09 43.3	+56 11.7	19.0	1626+1547	2	0.0299
25.	0943+563	09 43.8	+56 20.8	17.5	1337	2	0.0261
26.	0948+532	09 48.2	+53 14.6	18.0	715	2	0.0465
27.	1001+555	10 01.3	+55 34.0	18.0	723+ 774	4	0.0039
28.	1011+601A	10 11.5	+60 05.4	17.5	987+1005	4	0.0078
29.	1011+600B	10 11.6	+60 04.3	17.5	702+ 700	4	0.0073
30.	1017+542	10 17.2	+54 15.4	18.5	1114+ 739	2	0.0303
31.	Mkn 1434	10 30.9	+58 19.3	16.5	1061+1053	2	0.0082
32.	1033+531	10 33.5	+53 06.7	17.0	1153+1161	2	0.0038
33.	1037+494	10 37.7	+49 28.0	18.0	1202+1237	2	0.0052
34.	1047+598	10 47.8	+59 47.9	17.5	955+ 955	4	0.0853
35.	1055+597	10 55.7	+59 44.9	18.0	688	4	0.0235
36.	1106+500	11 06.4	+50 03.6	17.0	1083	2	0.0473
37.	1114+587	11 14.2	+58 46.7	17.5	1779	2	0.0056
38.	1116+583B	11 16.6	+58 19.8	19.5	2467+2477	2	0.0336
39.	1118+578B	11 18.9	+57 51.4	16.5	705+ 725	4	0.0073
40.	1118+587	11 18.8	+58 45.3	17.0:	1058+1097	4	0.0284
41.	1119+601	11 19.3	+60 08.0	17.5	551	2	0.0112
42.	1122+575	11 22.3	+57 31.6	17.5	1097+1082	4	0.0045
43.	1122+610	11 22.4	+61 02.8	17.0:	743+ 670	4	0.0325
44.	1123+576	11 23.4	+57 36.7	16.5	715+ 686	4	0.0014
45.	1124+580	11 24.7	+57 59.9	17.5	740	4	0.0194
46.	Mkn 1448	11 32.0	+50 22.0	17.0	1345+1345	2	0.0260
47.	Mkn 1450	11 35.8	+58 09.1	15.5	497	4	0.0033
48.	1147+520	11 47.3	+52 00.6	16.5	1212	2	0.0036

Table 1—(*continued*)

1	2	3	4	5	6	7	8
49.	1149+579	11 49.4	+57 57.7	17.5	912	2	0.0319
50.	1149+596	11 50.0	+59 39.2	18.5	734+ 715	2	0.0112
51.	1159+545	11 59.5	+54 31.9	18.0	1443+1510	2	0.0122
52.	1205+557	12 06.0	+55 41.8	15.5	1100+1048	2	0.0062
53.	1211+540	12 11.6	+54 02.0	18.0	1583+1563	2	0.0032
54.	1212+563	12 12.3	+56 21.8	19.5	1506+1404	2	0.0482
55.	1221+545B	12 22.0	+54 30.4	17.0:	636+ 566	4	0.0189
56.	1222+588	12 22.5	+58 48.6	18.0	759	2	0.0157
57.	1249+493	12 49.6	+49 18.8	17.5	1702+1704	2	0.0255
58.	1305+542	13 05.0	+54 12.6	17.0	1053	2	0.0298
59.	1305+547	13 05.4	+54 41.7	15.5	1157+1090	2	0.0324
60.	1307+563	13 07.7	+56 17.4	18.0	773+ 764	2	0.0172
61.	1319+579A	13 19.4	+57 56.8	18.5	981+ 950	2	0.0077
62.	1319+579B	13 19.4	+57 56.7	18.5	1373+1338	2	0.0069
63.	Mkn 1481	13 41.1	+52 56.4	17.0	1100	2	0.0063
64.	1342+562A	13 31.5	+56 16.8	17.0	1079+1049	2	0.0707
65.	1342+562B	13 42.6	+56 16.6	17.5	1103	2	0.0704
66.	Mkn 1486	13 58.1	+57 40.9	17.5	1139+ 604	2	0.0338
67.	1408+551B	14 08.7	+55 07.1	17.5	1214	2	0.0403
68.	1408+551A	14 08.2	+55 10.4	17.5	980+1320	2	0.0778
69.	1423+518	14 23.7	+51 45.6	18.0	1170	2	0.0072
70.	1430+521	14 30.3	+52 05.1	17.5	1124+1124	2	0.0257
71.	1432+530	14 32.7	+53 01.3	17.5	1120+1120	2	0.0451
72.	Mkn 826	14 48.5	+52 36.7	15.0	815	2	0.0000
73.	1457+540	14 57.1	+54 02.8	17.5	1160	2	0.0269
74.	1520+572	15 20.1	+57 14.3	17.0:	582	2	0.0721

Table 1—(*continued*)

1	2	3	4	5	6	7	8
75.	1522+588	15 22.7	+58 52.4	17.0:	2016	2	0.0338
76.	1524+575A	15 24.5	+57 33.9	17.0:	954	4	0.0304
77.	1524+575B	15 24.7	+57 33.9	17.0:	2349	2	0.0402
78.	1524+589	15 24.2	+58 56.0	17.0:	1168	4	0.0596
79.	1526+585B	15 26.0	+58 34.9	17.0:	1075+1090	4	0.0304
80.	1527+583	15 27.4	+58 20.9	18.0	802	4	0.0210
81.	Mkn 483	15 28.7	+34 05.7	17.0	1229+1246	2	0.0484
82.	1532+585B	15 32.9	+58 30.5	17.5	986+ 990	2	0.1093
83.	1533+574B	15 33.0	+57 26.5	17.0:	1115	2	0.0113

Absolute magnitude M_B was calculated from the apparent magnitude in the B band given in Table 2. For these galaxies which have no photometric observations, the absolute magnitude has been calculated using the photographic apparent magnitude given in Table 1.

Electron temperature T_e was calculated from the ratio of [OIII] $\lambda 4959 + 5007$ Å and [OIII] $\lambda 4363$ Å line intensities (Aller, 1984) for those galaxies where the line [OIII] $\lambda 4363$ Å is observed. For the rest of the galaxies, the electron temperature has been evaluated using empirical relationship between electron temperature and the total intensity of the lines [OIII] $\lambda 3727$ Å and [OIII] $\lambda 4959 + 5007$ Å (Pagel *et al.*, 1979).

As a rule, we obtained spectra only in the blue region. Therefore the adopted value for the electron density N_e is $100\ \mathrm{cm}^{-3}$, being typical for the BCDGs.

The relative concentrations of ions have been calculated according to the formulae given in Aller (1984). To calculate the element abundances, the unobserved ionization stages have been taken into account by means of correcting factors (French, 1981, Perrinotto, 1983 and Gonzales-Riestra *et al.*, 1988):

$$\frac{\mathrm{O}}{\mathrm{H}} = \frac{\mathrm{O}^+ + \mathrm{O}^{2+}}{\mathrm{H}^+}, \tag{1}$$

$$\frac{\mathrm{Ne}}{\mathrm{H}} = \frac{\mathrm{Ne}^{2+}}{\mathrm{H}^+} \frac{1}{1.2\,\mathrm{O}^{2+}/\mathrm{O} - 0.2}, \tag{2}$$

$$\frac{\mathrm{S}}{\mathrm{H}} = \frac{1}{4} \frac{\mathrm{S}^+}{\mathrm{H}^+} \frac{\mathrm{O}}{\mathrm{O}^+}, \tag{3}$$

$$\frac{\mathrm{N}}{\mathrm{H}} = \frac{\mathrm{N}^+}{\mathrm{H}^+} \frac{\mathrm{O}}{\mathrm{O}^+}, \tag{4}$$

$$\frac{\mathrm{He}}{\mathrm{H}} = \frac{\mathrm{He}^+}{\mathrm{H}^+} \frac{1}{1 - 0.25\,\mathrm{O}^+/\mathrm{O}}. \tag{5}$$

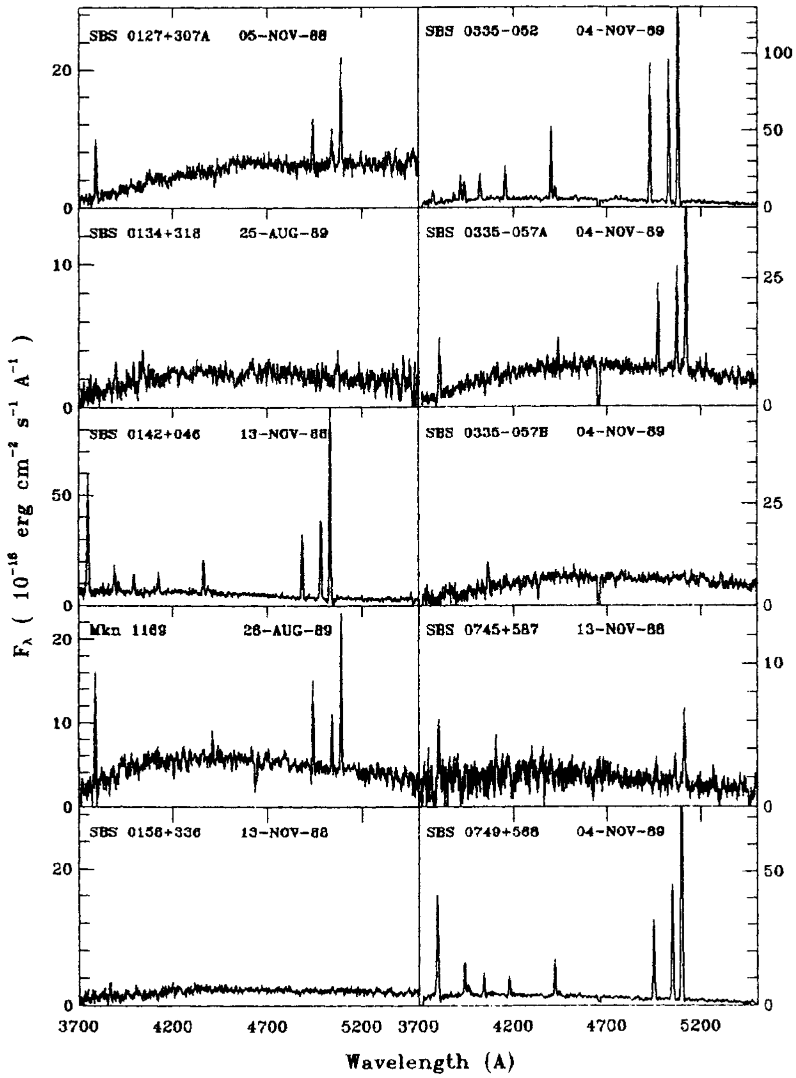

Figure 1 Spectra of galaxies uncorrected for extinction.

The T_e values, relative ions concentrations, and the abundances of the heavy elements are also given in Table 3.

4. GENERAL CHARACTERISTICS OF THE SAMPLE

To illustrate the depth of the SBS sample, the distribution of the magnitudes m_{pg} for our sample is shown in Figure 2c. Most galaxies (67 from 83) have the m_{pg}

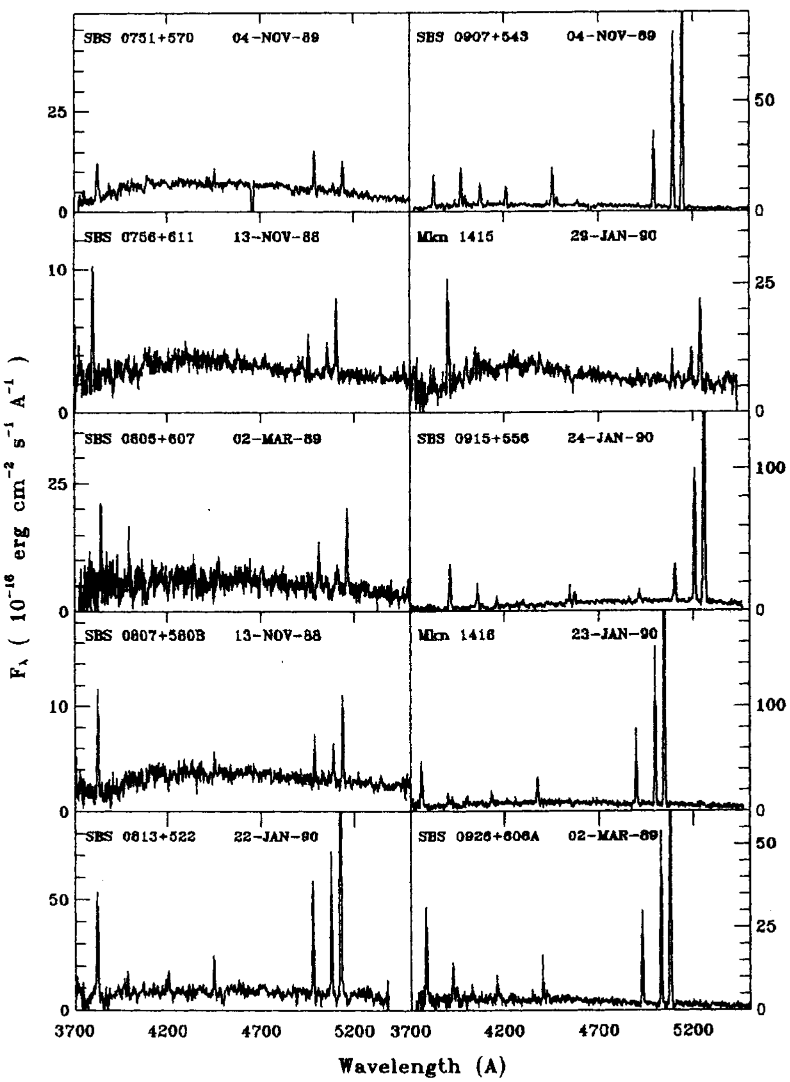

Figure 1 Spectra of galaxies uncorrected for extinction.

magnitudes in the range from 17.0 to 18.5. Also shown in Figures 2a and 2b are the apparent magnitude distribution for 155 galaxies in the UM survey (Salzer *et al.*, 1989) and the magnitude distribution for 1489 objects in the Markarian survey (Mazzarella and Balzano, 1986). The comparison of the magnitude distribution of the three surveys suggests that the SBS sample is substantially deeper than the Markarian survey but the weak tail of our sample coincides with UM galaxies. The galaxies with $m < 15^m$ are absent in this sample of SBS galaxies.

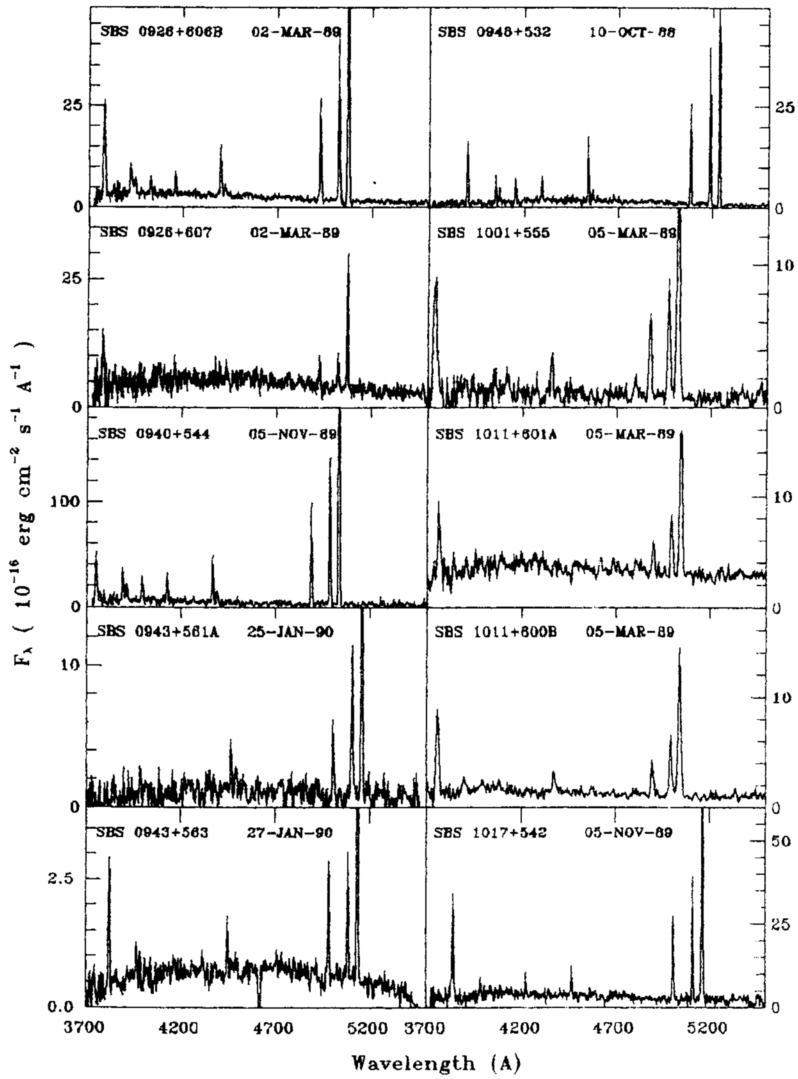

Figure 1 Spectra of galaxies uncorrected for extinction.

The distribution of possible BCDGs over the observed redshift is shown in Figure 3c. For the majority of the galaxies (64 from 83), the distance to the Sun is below 200 Mpc ($z \leq 0.035$). The redshift distribution decreases over the range $z = 0.015$–0.025. This is probably a consequence of a void at these redshifts. Figures 3a and 3b show, for the sake of comparison, the redshift distribution for UM galaxies (Salzer *et al.*, 1989) and Markarian galaxies (Markarian *et al.*, 1989), respectively. The relatively large number of distant galaxies is observed in our sample as compared to the Markarian and UM galaxies.

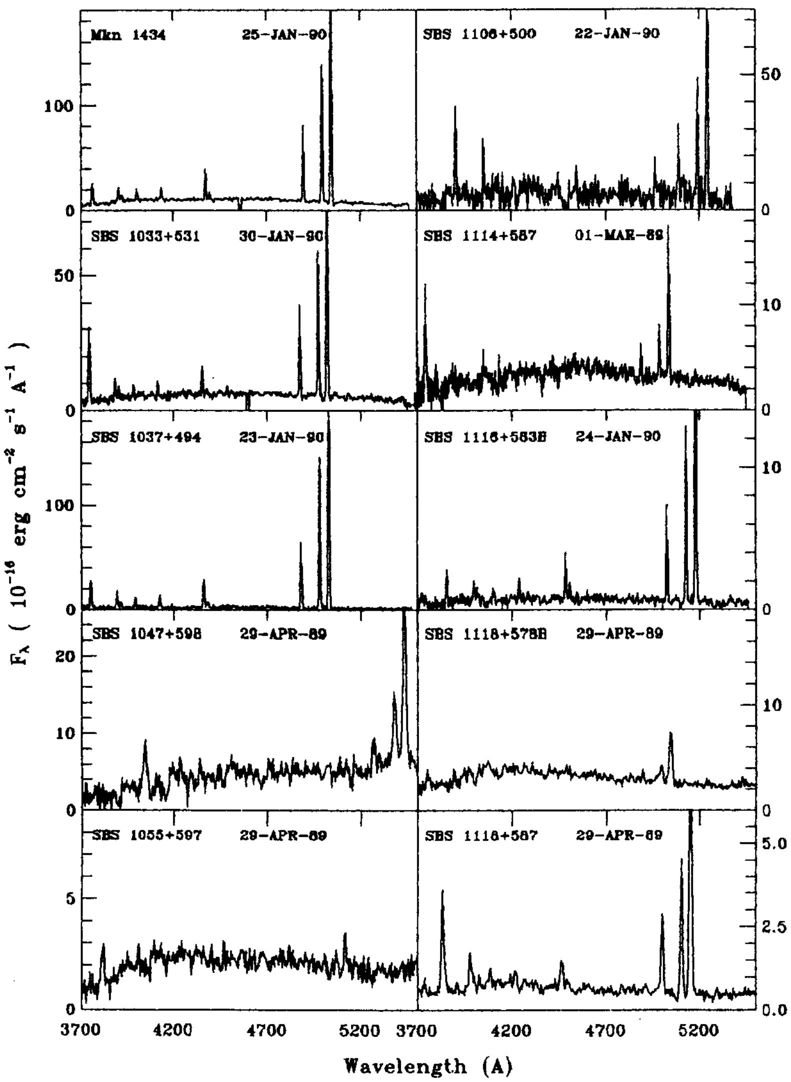

Figure 1 Spectra of galaxies uncorrected for extinction.

The distribution of absolute magnitudes M_B is given in Figure 4d. Usually, the BCDG definition has an upper limit for the total luminosity, $M_B \geq -17^m$–-18^m. A striking feature of the luminosity distribution of the galaxies from the SBS sample is a wide range of luminosities. The sample includes 40 galaxies more luminous than $M_B = -18^m$ which are assumed to be undergoing powerful starforming bursts. If we follow the accepted M_B limit, we shall omit many interesting objects (in Figure 7, the galaxies with $M_B \lesssim -18^m$ are marked with crosses). The galaxies on the right in Figure 4d are blue compact galaxies (BCGs)

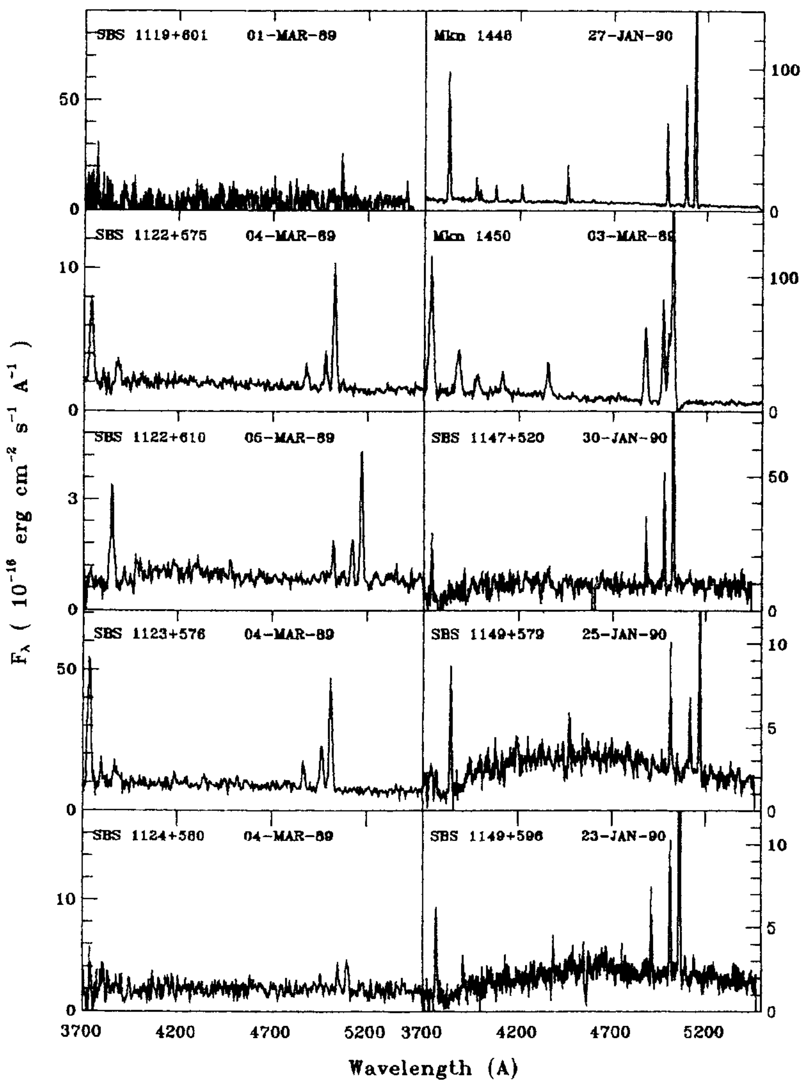

Figure 1 Spectra of galaxies uncorrected for extinction.

rather than blue compact dwarf galaxies (BCDGs). For comparison, in Figures 4a–c we plot the luminosity distributions for UM galaxies (Salzer *et al.*, 1989), Markarian galaxies (Mazzarella and Balzano, 1986) and a sample of normal galaxies from the UGC (Nilson, 1973; Zwicky *et al.*, 1961–1968). Twenty five per cent of galaxies in our sample have $M_B > -16.5$. This figure complies with the luminosity distribution of UM galaxies in this range. The luminosity distributions of Markarian and normal galaxies in the high-luminosity region are displaced with respect to our sample.

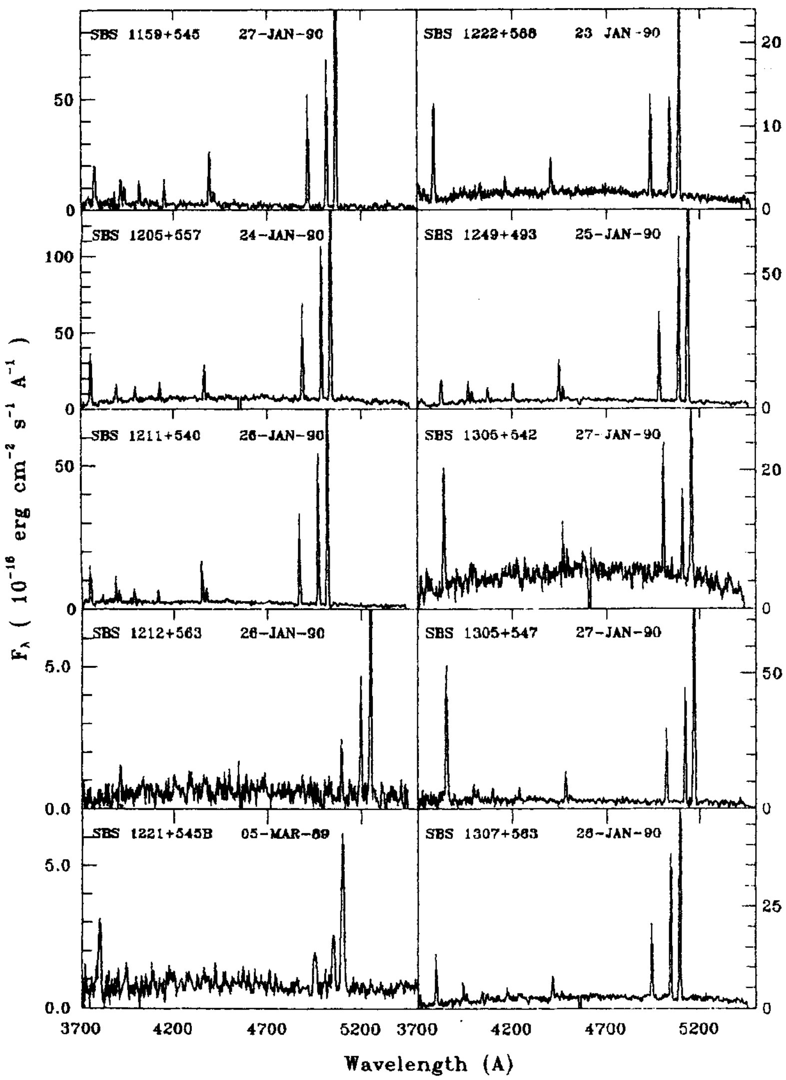

Figure 1 Spectra of galaxies uncorrected for extinction.

Figure 5d presents the oxygen abundance distribution of SBS galaxies. 25 galaxies have oxygen abundance less than 8.1 in 12 + log (O/H) units. Oxygen abundance distribution for the galaxies with correct abundance estimates, i.e., the galaxies for which T_e has been obtained from the [OIII] 4959 + 5007/4363 ratios (solid line in Figure 5d), are displaced toward the low-abundance region with respect to other distributions (Figure 5a; Skillman *et al.*, 1989; Figure 5b; Campbell *et al.*, 1986; Figure 5c; Kunth and Sargent, 1983).

Figures 6–9 show the oxygen abundance as a function of different parameters

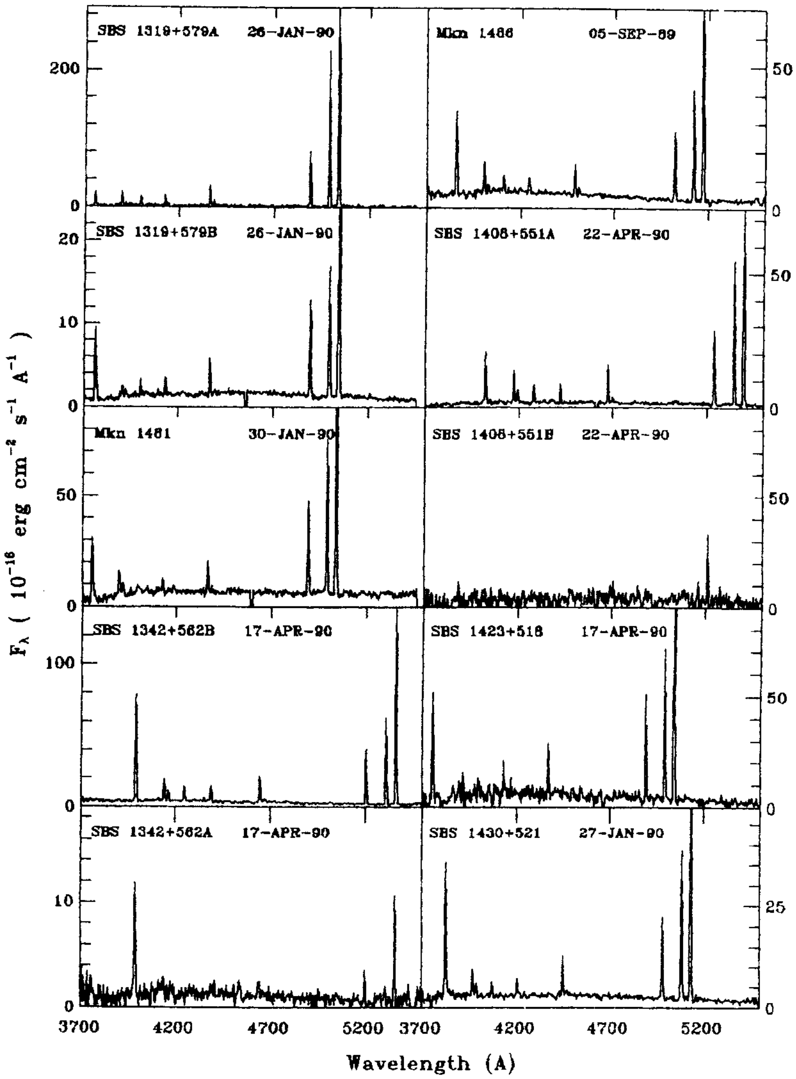

Figure 1 Spectra of galaxies uncorrected for extinction.

and Figure 10 shows the dependence of EW (H_β) on the logarithm of H_β luminosity for 74 galaxies. For 9 galaxies from Table 1, oxygen abundance has not been determined because of low intensities of emission lines (as low as the measurement errors).

As can be seen from Figure 6, the galaxies with lower heavy element abundance show small inner extinction coefficients c (H_β). The dispersion of the dots relative to c (H_β) increases with heavy element abundance increasing. This result is in close agreement with that obtained by Campbell *et al.* (1986).

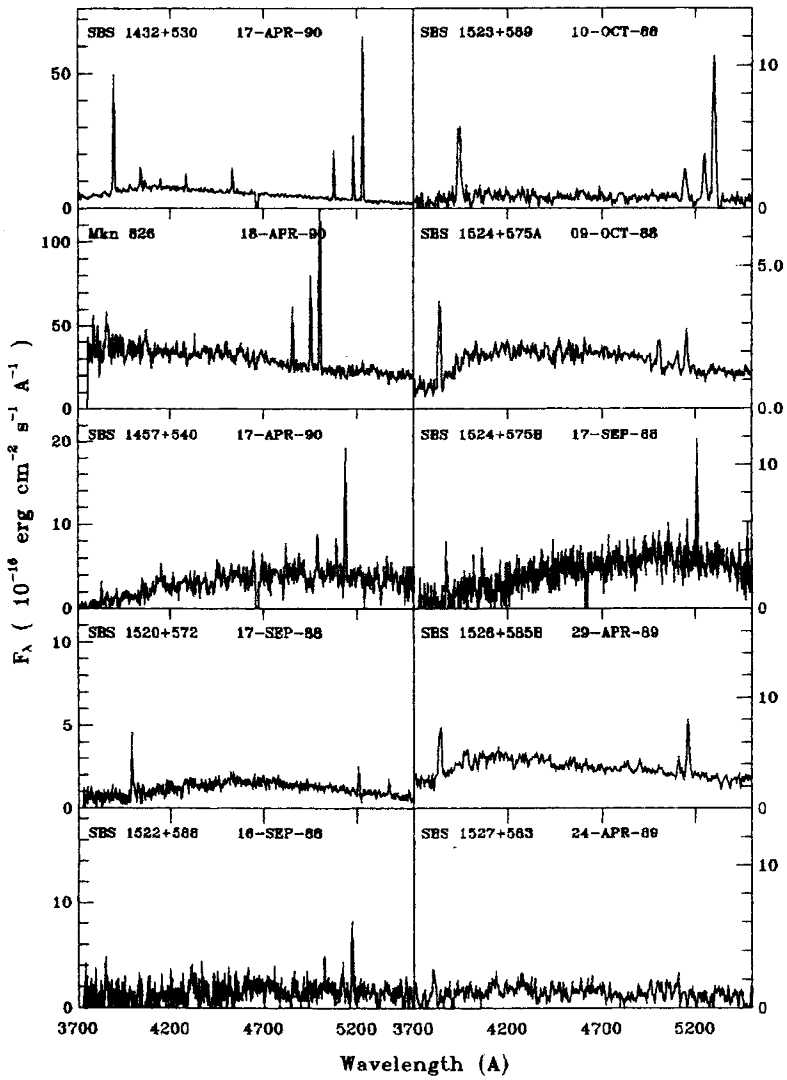

Figure 1 Spectra of galaxies uncorrected for extinction.

A strong correlation between oxygen abundance and T_e (Figure 7) is a consequence of their functional dependence (T_e can be determined from oxygen line intensity ratios by the above two methods). The galaxies with higher T_e ([OIII] λ4363 Å line is observed in their spectra) have the abundances less than $12 + \log(O/H) = 8.2$. These galaxies show less dispersion in T_e than those with $12 + \log(O/H) > 8.2$, where T_e is determined using Pagel's method (Pagel *et al.*, 1979). A striking feature of our sample is a large number of galaxies with extreme deficiency of oxygen (9 galaxies with $(O/H)/(O/H)_{\odot} < 1/20$).

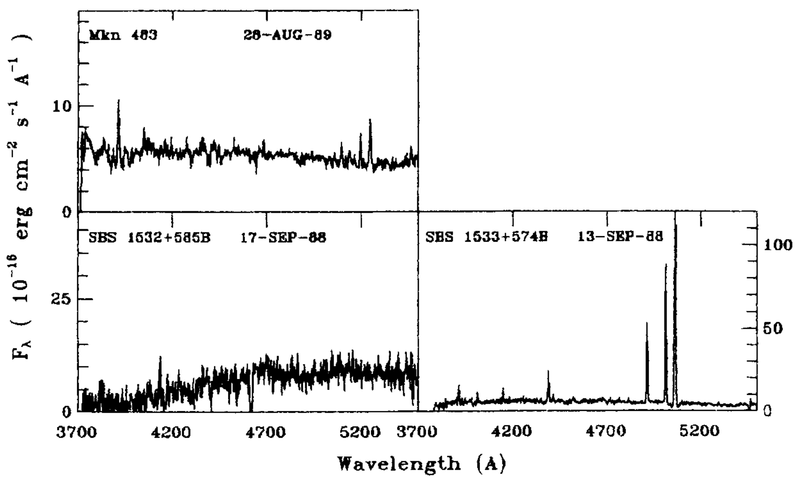

Figure 1 Spectra of galaxies uncorrected for extinction.

Figure 8 presents the relationship between H_β equivalent widths and oxygen abundance. The galaxies for which T_e are obtained from [OIII] $\lambda 4959+5007$/[OIII] $\lambda 4363$ ratios are marked by asterisk. There is a weak anticorrelation between EW (H_β) and heavy element abundance in Figure 8. If H_β equivalent width characterizes the galaxy age, then Figure 8 confirms a close relation between the age and heavy element abundance. A high dispersion of EW (H_β) in the high-abundance region $(12+\log(O/H)>8.2)$ may be explained by the following reasons:

1) Large errors of Pagel's method for determination of T_e;

2) The enrichment of interstellar medium due to the evolution of low-mass stars becomes weaker with the galaxy age because the relative growth of heavy element abundance slows down in enriched medium;

3) Lack of a rigorous criterion for selection of galaxies with powerful starforming bursts. The criteria for their selection were the BCDG morphology and the availability of emission lines; we did not use the $EW_{5007} \geq 100$ Å selection criterion in this case. As follows from Figure 8, Pagel's method is probably inapplicable for BCDG chemical composition determination.

H_β absolute luminosity, $\log[L(H_\beta)]$, is plotted versus oxygen abundance in Figure 9. The galaxies for which T_e is determined from the I([OIII] $\lambda 4959+5007$)/I([OIII] $\lambda 4363$) ratio are marked by asterisk, and those for which T_e is determined by Pagel's method, are marked by triangles. There is no correlation of starforming burst power, characterised by H_β luminosity, with oxygen abundance. The reasons for the absence of such dependence can be as follows:

—the power of starbursts in the BCDGs is independent of the galaxy chemical composition. As shown by Izotov (1990), the formation of star forming regions at low heavy element abundances may be different from that in spiral galaxies. In this case rather molecular hydrogen than heavy elements is the main cooling agent which regulates the collapse of protostars. If we take into account that H_2

Table 2 Results of photoelectric observations

No.	Galaxy SBS	D	V	U–B	B–V	V–R
1	2	3	4	5	6	7
1.	0142+046	12"	16.70±0.04	−0.55±0.10	+0.14±0.03	0.54±0.05
2.	0335−052	12	16.42±0.03	−0.12±0.09	+0.32±0.03	0.65±0.04
3.	0335−057A	12	16.78±0.05	+0.27±0.16	+0.55±0.05	0.88±0.04
4.	0335−057B	12	16.96±0.06	+0.32±0.19	+0.49±0.05	0.51±0.05
5.	0749+568	12	16.79±0.07	−0.02±0.19	+0.56±0.06	0.81±0.06
6.	0751+570	12	16.46±0.06	+0.17±0.17	+0.31±0.05	0.57±0.05
7.	0813+522	12	16.19±0.04	−0.41±0.13	+0.36±0.04	0.41±0.10
8.	0907+543	12	16.88±0.07	+0.17±0.14	+0.55±0.07	0.74±0.07
9.	0915+556	12	16.30±0.03	+0.15±0.13	+0.78±0.04	0.89±0.03
10.	Mkn 1416	12	16.64±0.03	−0.16±0.11	+0.09±0.03	0.44±0.03
11.	0926+606	12	15.81±0.03	+0.04±0.08	+0.16±0.03	0.31±0.06
12.	0926+607	12	16.44±0.03	+0.19±0.16	+0.53±0.05	0.72±0.07
13.	0940+544	12	17.25±0.08	−0.27±0.16	+0.10±0.06	0.31±0.06
14.	0943+561A	12	18.42±0.06	−0.26±0.21	+0.16±0.05	0.42±0.05
15.	0943+563	9	18.06±0.13	+0.04±0.20	+0.66±0.20	0.85±0.20
16.	1011+601A	9	17.18±0.03	−0.05±0.08	+0.22±0.02	0.40±0.04
17.	1011+600B	9	17.47±0.03	+0.15±0.16	+0.36±0.04	0.37±0.04
18.	1017+542	12	17.83±0.06	−0.03±0.17	+0.47±0.05	0.75±0.05
19.	1037+494	12	17.08±0.04	−0.05±0.03	+0.20±0.11	0.53±0.03
20.	1047+598	9	16.86±0.02	−0.04±0.09	+0.37±0.04	0.34±0.05
21.	1055+597	9	17.28±0.03	+0.47±0.11	+0.96±0.05	0.93±0.05
22.	1116+583B	12	18.58±0.06	+0.25±0.19	+0.41±0.06	0.64±0.06
23.	1118+578B	9	16.64±0.03	−0.17±0.09	+0.41±0.06	0.16±0.04

Table 2—(*continued*)

1	2	3	4	5	6	7
24.	1118+587	9	17.97±0.06	−0.19±0.12	+0.59±0.08	0.60±0.06
25.	1122+610	9	17.64±0.04	+0.02±0.07	+0.57±0.05	0.63±0.04
26.	1123+576	9	15.92±0.03	−0.17±0.08	+0.31±0.04	0.59±0.04
27.	Mkn 1448	12	16.77±0.02	−0.25±0.10	−0.03±0.03	0.48±0.03
28.	1149+579	12	17.17±0.09	−0.03±0.18	+0.51±0.07	0.59±0.04
29.	1221+545B	9	17.76±0.06	−0.43±0.14	+0.61±0.07	0.53±0.09
30.	1305+547	12	17.64±0.04	−0.35±0.08	−0.11±0.03	0.41±0.03
31.	Mkn 1481	12	16.35±0.02	−0.18±0.07	+0.51±0.03	0.67±0.03
32.	1342+562A	12	16.79±0.04	−0.11±0.12	+0.40±0.04	0.70±0.04
33.	1342+562B	8	17.86±0.08	+0.24±0.18	+0.62±0.12	0.84±0.11
34.	Mkn 1486	12	16.56±0.04	+0.18±0.19	+0.40±0.05	0.65±0.04
35.	1423+518	12	17.32±0.03	−0.20±0.06	+0.25±0.03	0.43±0.03
36.	1432+530	12	16.67±0.03	−0.17±0.09	+0.05±0.03	0.35±0.04
37.	1526+585B	9	17.18±0.04	−0.29±0.07	+0.30±0.06	0.36±0.05

formation in the gas deficient of heavy elements is determined mostly by abundances of H^- and H_2^+ ions, we can conclude that there may be only a weak correlation between H_β luminosity and oxygen abundance;

—the bursts of star formation in different galaxies start at approximately the same heavy element abundance and the observed spread in oxygen abundance is a consequence of HII gas enrichment by the products of stellar evolution.

The plot of H_β equivalent width vs H_β luminosity is shown in Figure 10. As in Figure 9, the galaxies with emission line [OIII] λ4363 are marked by asterisks. As follows from Figure 10, the mean H_β luminosity of these galaxies is higher than that in the galaxies without [OIII] λ4363 line. The former galaxies have larger equivalent widths as well. The separation between these two samples plotted in Figure 10 is due to their different ages because both EW (H_β) and L (H_β) are functions of star burst ages.

5. CONCLUSIONS

The main results of the present paper are as follows:

1. The chemical composition of 79 possible blue compact dwarf galaxies from the Second Byurakan Survey has been determined. The sample contains a large number of galaxies with extremely low heavy element abundance.

Table 3 Results of spectrophotometric observations

Line	λ_o	Galaxy			
		0127+307A	0142+046	Mkn 1169	0335−052
[OII]	3727	3.396±0.278	1.237±0.176	1.193±0.371	0.268±0.009
[NeIII]	3868	–	0.346±0.050	–	0.203±0.008
HeI+H_8	3887	–	0.197±0.031	–	0.177±0.007
[NeIII]+H_ε	3968	–	0.231±0.031	–	0.208±0.007
H_δ	4102	–	0.292±0.036	–	0.270±0.009
H_γ	4340	–	0.468±0.041	0.431±0.088	0.484±0.014
[OIII]	4363	–	0.104±0.011	–	0.121±0.005
HeI	4471	–	–	–	0.037±0.002
HeII	4686	–	–	–	0.028±0.002
[ArIV]	4712	–	–	–	0.015±0.002
H_β	4861	1.000	1.000	1.000	1.000
[OIII]	4959	0.832±0.093	1.187±0.045	0.663±0.062	1.001±0.026
[OIII]	5007	2.034±0.184	3.415±0.150	1.834±0.154	2.883±0.061
HeI	5876	–	–	–	0.128±0.006
H_α	6563	2.943±0.248	–	–	2.631±0.053
[SII]	6717+6731	–	–	–	0.011±0.001
$c(H_\beta)$		0.000±0.109	0.239±0.140	0.383±0.328	0.000±0.026
$EW(H_\beta)$		11	123	17	172
d, Mpc		103	34	99	84
M_B		−18.06	−16.50	−17.98	−16.40
$L(H_\beta)$, $erg \cdot s^{-1}$		$7.47 \cdot 10^{39}$	$1.21 \cdot 10^{40}$	$8.54 \cdot 10^{39}$	$5.71 \cdot 10^{40}$
T_e, K		9900±830	19020±1580	8070±630	22900±2300
$O^+/H^+ (*10^{-6})$		136.4±74.0	5.599±1.738	124.8±101.3	0.773±0.202
$O^{2+}/H^+ (*10^{-5})$		8.043±3.816	2.134±0.621	14.62±7.21	1.260±0.320
$Ne^{2+}/H^+ (*10^{-6})$		–	4.560±1.298	–	1.780±0.490
$Ar^{3+}/H^+ (*10^{-8})$		–	–	–	6.220±2.030
$S^+/H^+ (*10^{-9})$		–	–	–	4.910±1.760
He^+/H^+		–	–	–	0.085±0.006
12+log(O/H)		8.34±0.23	7.44±0.06	8.46±0.06	7.12±0.25
12+log(Ne/H)		–	6.90±0.17	–	6.28±0.28
12+log(Ar/H)		–	–	–	4.79±0.28
12+log(S/H)		–	–	–	4.93±0.36
12+log(He/H)		–	–	–	10.93±0.07

Table 3—(*continued*)

Line	λ_o	Galaxy			
		0335−057A	0749+568	0807+580B	0813+522
[OII]	3727	0.761±0.095	1.364±0.034	2.064±0.171	2.389±0.576
[NeIII]	3868	0.150±0.024	0.446±0.014	0.259±0.037	0.358±0.094
HeI+H_8	3887	–	0.144±0.006	–	0.214±0.058
[NeIII]+H_ϵ	3968	–	0.250±0.010	–	0.195±0.049
H_δ	4102	–	0.264±0.010	–	0.317±0.068
H_γ	4340	0.397±0.044	0.480±0.014	0.558±0.064	0.470±0.074
[OIII]	4363	–	0.061±0.003	–	–
HeI	4471	–	0.047±0.003	–	–
H_β	4861	1.000	1.000	1.000	1.000
[OIII]	4959	1.152±0.076	1.559±0.122	1.066±0.102	1.335±0.090
[OIII]	5007	3.906±0.210	4.741±0.161	2.075±0.172	3.583±0.226
H_α	6563	2.859±0.323	2.750±0.084	2.798±0.218	–
[NII]	6584	0.050±0.001	0.093±0.010	–	–
[SII]	6717	0.390±0.067	–	2.216±0.181	–
[SII]	6732	0.390±0.067	–	–	–
$c(H_\beta)$		0.118±0.073	0.000±0.094	0.000±0.296	0.805±0.255
$EW(H_\beta)$		23	135	12	65
d,Mpc		135	110	160	145
M_B		−19.78	−18.38	−18.51	−18.80
$L(H_\beta)$, erg·s^{-1}		$6.77\cdot10^{40}$	$6.83\cdot10^{40}$	$9.63\cdot10^{39}$	$6.96\cdot10^{40}$
T_e, K		9640±800	12670±460	9260±760	10430±890
$O^+/H^+(*10^{-6})$		34.23±20.21	20.97±4.01	111.3±61.9	77.09±50.86
$O^{2+}/H^+(*10^{-5})$		16.68±7.31	8.455±1.551	11.06±5.24	11.66±4.701
$Ne^{2+}/H^+(*10^{-6})$		16.98±10.26	18.26±3.51	34.84±20.84	29.52±19.63
$S^+/H^+(*10^{-6})$		1.803±0.881	–	5.704±2.294	–
He^+/H^+		–	0.099±0.07	–	–
12+log(O/H)		8.31±0.06	8.03±0.06	8.35±0.22	8.29±0.22
12+log(Ne/H)		7.43±0.17	7.49±0.17	7.94±0.26	7.75±0.29
12+log(S/H)		6.42±0.21	–	7.06±0.18	–
12+log(He/H)		–	10.99±0.03	–	–

Table 3—(*continued*)

Line	λ_o	Galaxy			
		0907+543	Mkn 1415	0915+556	Mkn 1416
[OII]	3727	0.488±0.040	4.020±0.258	2.886±0.603	1.256±0.236
H_9	3832	0.064±0.008	-	-	-
[NeIII]	3868	0.555±0.044	-	1.200±0.235	0.277±0.054
HeI+H_8	3887	0.140±0.014	-	0.207±0.049	-
[NeIII]+H_ε	3968	0.349±0.030	-	0.431±0.086	0.191±0.038
H_δ	4102	0.288±0.025	-	0.286±0.054	0.270±0.044
H_γ	4340	0.548±0.044	-	0.470±0.065	0.470±0.056
[OIII]	4363	0.104±0.011	-	0.400±0.056	0.051±0.009
HeII	4686	-	-	0.346±0.031	-
H_β	4861	1.000	1.000	1.000	1.000
[OIII]	4959	2.386±0.235	1.365±0.103	3.073±0.146	1.932±0.089
[OIII]	5007	7.327±0.601	3.332±0.218	8.784±0.414	5.477±0.243
H_α	6563	2.750±0.253	-	-	-
c(H_β)		0.000±0.258	-	1.402±0.222	0.796±0.193
EW(H_β)		154	6	44	95
d,Mpc		165	283	295	46
M_B		-19.08	-20.76	-19.85	-16.31
L(H_β),erg·s^{-1}		$1.53\cdot10^{41}$	$3.62\cdot10^{40}$	$2.12\cdot10^{41}$	$1.16\cdot10^{40}$
T_e, K		13160±1010	11040±230	24280±3350	11190±840
$O^+/H^+(*10^{-5})$		0.649±0.276	10.34±1.752	0.756±0.482	3.068±1.730
$O^{2+}/H^+(*10^{-5})$		11.06±4.13	9.346±1.451	3.965±1.669	14.16±5.039
$Ne^{2+}/H^+(*10^{-6})$		11.13±4.58	-	9.367±5.747	17.52±9.770
He^+/H^+		0.156±0.019	-	-	-
12+log(O/H)		8.07±0.06	8.29±0.07	7.67±0.20	8.24±0.17
12+log(Ne/H)		7.09±0.17	-	7.06±0.27	7.35±0.24

2. The comparison with other samples of emission-line galaxies shows that the galaxy sample from SBS is one of the deepest ones.

The results of the spectrophotometric observations of blue compact dwarf galaxies obtained in this paper represent only the first part of the chemical composition study of total BCDG sample from the Second Byurakan Survey, which is in progress now and will be published later.

The authors would like to thank L. K. Erastova for her assistance in taking sample galaxies and advise. We are also indebted to A. I. Shapovalova, I. S. Balinskaya, and S. A. Pustil'nick for assisting in carrying of the observations.

Table 3—(*continued*)

Line	λ_o	Galaxy			
		0926+606A	0926+606B	0940+544	0943+563
[OII]	3727	1.272±0.113	1.216±0.048	0.538±0.021	2.976±0.448
[NeIII]	3868	0.336±0.059	0.429±0.023	0.320±0.014	0.429±0.073
HeI+H_8	3887	0.155±0.019	0.178±0.012	0.182±0.009	–
[NeIII]+H_ε	3968	0.106±0.015	0.215±0.014	0.258±0.011	0.447±0.076
H_δ	4102	0.309±0.030	0.247±0.015	0.269±0.011	–
H_γ	4340	0.462±0.038	0.550±0.027	0.476±0.016	0.464±0.064
[OIII]	4363	0.119±0.015	0.139±0.011	0.122±0.007	–
HeI	4471	–	–	0.040±0.003	–
H_β	4861	1.000	1.000	1.000	1.000
[OIII]	4959	1.685±0.081	1.712±0.063	1.479±0.038	1.443±0.115
[OIII]	5007	4.554±0.189	4.368±0.135	4.214±0.089	3.913±0.271
HeI	5876	0.191±0.021	–	0.124±0.010	–
H_α	6563	2.859±0.231	–	2.755±0.105	2.859±0.486
[NII]	6584	0.079±0.012	–	–	–
[SII]	6717	0.208±0.031	–	–	–
[SII]	6732	0.181±0.023	–	–	–
$c(H_\beta)$		0.165±0.052	0.000±0.158	0.000±0.049	0.157±0.110
$EW(H_\beta)$		151	140	345	35
d,Mpc		82	80	34	157
M_B		−17.07	−17.01	−15.69	−18.97
$L(H_\beta)$, erg·s^{-1}		$2.03 \cdot 10^{40}$	$1.79 \cdot 10^{40}$	$1.73 \cdot 10^{40}$	$1.44 \cdot 10^{40}$
T_e, K		17100±1500	18170±1120	18200±800	10880±940
$O^+/H^+ (*10^{-6})$		7.715±3.258	6.200±1.641	2.720±0.544	80.88±47.96
$O^{2+}/H^+ (*10^{-5})$		3.842±1.254	3.370±0.758	2.960±0.473	11.12±4.86
$Ne^{2+}/H^+ (*10^{-6})$		5.754+2.871	6.310±1.717	4.691±0.937	30.06±17.94
$N^+/H^+ (*10^{-7})$		4.744±1.896	–	–	–
$S^+/H^+ (*10^{-7})$		2.617±1.005	–	–	–
He^+/H^+		0.160±0.021	–	0.088±0.007	–
12+log(O/H)		7.66±0.15	7.60±0.10	7.51±0.06	8.28±0.22
12+log(Ne/H)		6.86±0.22	6.89±0.11	6.75±0.17	7.78±0.26
12+log(S/H)		6.20±0.17	–	–	–
12+log(N/H)		6.45±0.17	–	–	–
12+log(He/H)		11.20±0.06	–	10.95±0.08	–

Table 3—(*continued*)

Line	λ_o	Galaxy			
		0948+532	1011+601A	1017+542	Mkn 1434
[OII]	3727	0.877±0.067	3.043±0.647	1.826±0.392	0.450±0.051
[NeIII]	3868	0.303±0.025	0.555±0.120	0.290±0.065	0.285±0.031
HeI+H_8	3887	0.127±0.012	–	–	0.129±0.015
[NeIII]+H_ε	3968	0.234±0.019	0.386±0.106	–	0.198±0.021
HeI	4026	0.060±0.008	–	–	–
[SII]	4069	0.053±0.006	–	–	–
H_δ	4102	0.254±0.019	–	0.292±0.057	0.254±0.023
H_γ	4340	0.470±0.027	0.722±0.127	0.468±0.056	0.470±0.031
[OIII]	4363	0.066±0.006	–	–	0.103±0.009
HeI	4471	0.057±0.006	–	–	–
H_β	4861	1.000	1.000	1.000	1.000
[OIII]	4959	1.741±0.050	1.740±0.187	1.307±0.081	1.786±0.050
[OIII]	5007	5.014±0.128	4.408±0.407	3.805±0.220	4.268±0.113
HeI	5876	0.111±0.009	–	–	–
H_α	6563	2.893±0.190	2.859±0.689	–	–
[NII]	6584	0.032±0.004	–	–	–
[SII]	6717+6731	0.174±0.015	–	–	–
$c(H_\beta)$		0.735±0.057	0.251±0.156	0.413±0.226	0.551±0.106
$EW(H_\beta)$		192	54	117	76
d, Mpc		279	44	182	49
M_B		−19.23	−15.72	−18.49	−16.95
$L(H_\beta)$, erg·s^{-1}		$1.78\cdot10^{41}$	$1.56\cdot10^{39}$	$1.42\cdot10^{41}$	$1.87\cdot10^{40}$
T_e, K		12704±570	11220±980	10250±870	15290±810
$O^+/H^+(*10^{-5})$		1.317±0.374	7.350±4.772	6.328±4.230	0.374±0.123
$O^{2+}/H^+(*10^{-5})$		8.459±1.687	11.65±5.33	13.79±5.96	5.352±1.119
$Ne^{2+}/H^+(*10^{-5})$		1.235±0.350	3.480±2.218	2.560±1.680	0.659±0.210
$S^+/H^+(*10^{-7})$		2.116±0.492	–	–	–
$N^+/H^+(*10^{-7})$		3.518±0.961	–	–	–
He^+/H^+		0.120±0.014	–	–	–
12+log(O/H)		7.99±0.09	8.28±0.23	8.32±0.06	7.76±0.09
12+log(Ne/H)		7.17±0.12	7.81±0.28	7.90±0.36	6.86±0.14
12+log(S/H)		6.20±0.10	–	–	–
12+log(N/H)		6.42±0.12	–	–	–
12+log(He/H)		11.08±0.05	–	–	–

Table 3—(*continued*)

Line	λ_o	Galaxy			
		1033+531	1037+494	1106+500	1116+583B
[OII]	3727	2.260±0.255	0.467±0.058	1.349±0.077	0.356±0.066
[NeIII]	3868	0.436±0.046	0.268±0.031	0.681±0.055	0.252±0.044
HeI+H_8	3887	0.210±0.024	0 098±0.013	–	0.156±0.029
[NeIII]+H_ε	3968	0.228±0.024	0.180±0.021	–	0.160±0.028
H_δ	4102	0.301±0.026	0.218±0.022	–	0.243±0.036
H_γ	4340	0.445±0.028	0.470±0.035	–	0.470±0.051
[OIII]	4363	0.048±0.006	0.098±0.010	–	0.145±0.020
H_β	4861	1.000	1.000	1.000	1.000
[OIII]	4959	1.450±0.041	2.108±0.064	1.588±0.084	1.844±0.084
[OIII]	5007	4.222±0.109	5.488±0.161	3.512±0.125	5.298±0.231
c(H_β)		1.099±0.137	0.048±0.118	–	0.076±0.175
EW(H_β)		52	263	69	104
d,Mpc		23	31	284	202
M_B		−14.81	−14.49	−20.26	−17.03
L(H_β),erg·s^{-1}		$1.87\cdot10^{39}$	$7.16\cdot10^{39}$	$2.11\cdot10^{41}$	$1.81\cdot10^{40}$
T_e, K		10570±510	13900±770	10000±150	17670±1720
$O^+/H^+(*10^{-5})$		13.49±4.938	0.520±0.189	5.190±0.729	0.194±0.106
$O^{2+}/H^+(*10^{-5})$		12.87±3.025	7.938±2.754	13.84±1.513	3.916±1.385
$Ne^{2+}/H^+(*10^{-6})$		34.07±11.92	8.198±2.853	–	3.970±2.092
12+log(O/H)		8.42±0.13	7.93±0.15	8.28±0.05	7.61±0.16
12+log(Ne/H)		7.84±0.15	6.95±0.15	–	6.62±0.23

Table 3—(*continued*)

Line	λ_o	Galaxy			
		1118+587	1122+610	1123+576	Mkn 1448
[OII]	3727	1.464±0.157	5.407±0.876	12.338±1.94	1.472±0.127
[NeIII]	3868	0.511±0.060	–	–	0.339±0.030
HeI+H_8	3887	–	–	–	0.137±0.014
[NeIII]+H_ε	3968	0.253±0.034	–	–	0.191±0.016
H_δ	4102	0.248±0.032	–	–	0.233±0.018
H_γ	4340	0.480±0.048	0.558±0.084	0.464±0.077	0.470±0.026
[OIII]	4363	–	–	–	0.046±0.005
HeI	4471	–	–	–	0.052±0.004
H_β	4861	1.000	1.000	1.000	1.000
[OIII]	4959	1.596±0.096	1.051±0.102	1.917±0.160	1.500±0.037
[OIII]	5007	4.590±0.235	3.155±0.260	4.490±0.338	3.855±0.089
HeI	5876	0.175±0.024	–	–	–
H_α	6563	2.860±0.284	2.859±0.530	2.859±0.498	–
$c(H_\beta)$		0.169±0.064	0.527±0.120	0.942±0.113	0.301±0.090
$EW(H_\beta)$		76	20	18	116
d,Mpc		170	195	8.6	156
M_B		−19.16	−19.08	−13.18	−18.97
$L(H_\beta)$, erg·s^{-1}		$5.69 \cdot 10^{40}$	$1.94 \cdot 10^{40}$	$9.38 \cdot 10^{37}$	$1.11 \cdot 10^{41}$
T_e, K		10590±910	11370±1000	13680±1250	11820±560
$O^+/H^+(*10^{-5})$		4.444±2.466	12.39±7.38	14.83±8.27	2.920±0.920
$O^{2+}/H^+(*10^{-5})$		13.98±5.91	7.651±3.407	6.637±2.740	9.270±1.979
$Ne^{2+}/H^+(*10^{-5})$		3.975±2.182	–	–	1.757±0.544
He^+/H^+		–	–	–	0.108±0.009
12+log(O/H)		8.27±0.20	8.30±0.23	8.33±0.22	8.09±0.10
12+log(Ne/H)		7.75±0.24	–	–	7.39±0.13
12+log(He/H)		–	–	–	11.04±0.04

Table 3—(*continued*)

Line	λ_o	Galaxy			
		Mkn 1450	1149+596	1159+545	1205+557
[OII]	3727	1.904±0.314	1.480±0.458	0.534±0.088	1.237±0.199
H_9	3832	–	–	0.083±0.016	–
[NeIII]	3868	0.706±0.108	0.365±0.113	0.308±0.049	0.406±0.065
HeI+H_8	3887	–	–	0.176±0.029	–
[NeIII]+H_ϵ	3968	0.286±0.044	–	0.225±0.034	0.244±0.038
H_δ	4102	0.278±0.041	–	0.208±0.029	0.240±0.034
H_γ	4340	0.470±0.048	0.470±0.094	0.470±0.047	0.470±0.047
[OIII]	4363	–	–	0.130±0.020	0.076±0.012
HeI	4471	–	–	0.039±0.006	–
H_β	4861	1.000	1.000	1.000	1.000
[OIII]	4959	1.076±0.052	1.799±0.152	1.287±0.058	1.493±0.063
[OIII]	5007	3.098±0.161	4.354±0.354	3.632±0.149	4.397±0.173
HeI	5876	0.084±0.015	–	–	–
H_α	6563	2.868±0.487	–	–	–
[SII]6717+6731		0.171±0.041	–	–	–
$c(H_\beta)$		0.288±0.165	0.154±0.323	0.331±0.159	0.885±0.162
$EW(H_\beta)$		139	19	347	88
d,Mpc		20	67	73	37
M_B		−15.98	−15.64	−16.32	−17.35
$L(H_\beta)$, erg·s^{-1}		$5.15\cdot10^{39}$	$1.28\cdot10^{39}$	$3.01\cdot10^{40}$	$3.43\cdot10^{40}$
T_e, K		9800±820	10870±940	20520±2100	14220±1210
$O^+/H^+(*10^{-5})$		8.001±5.016	4.038±3.037	0.202±0.104	1.281±0.673
$O^{2+}/H^+(*10^{-5})$		12.13±5.220	14.23±6.370	2.017±0.692	5.519±1.909
$Ne^{2+}/H^+(*10^{-5})$		7.488±4.481	2.564±1.889	0.342±0.170	1.160±0.594
$S^+/H^+(*10^{-7})$		3.797±1.848	–	–	–
He^+/H^+		0.062±0.012	–	0.088±0.016	–
12+log(O/H)		8.30±0.22	8.26±0.22	7.35±0.16	7.83±0.17
12+log(Ne/H)		8.16±0.26	7.54±0.32	6.58±0.22	7.18±0.22
12+log(S/H)		5.98±0.21	–	–	–
12+log(He/H)		10.79±0.09	–	10.94±0.08	–

Table 3—(*continued*)

Line	λ_o	Galaxy			
		1211+540	1221+545B	1222+588	1249+493
[OII]	3727	0.449±0.017	1.947±0.355	1.561±0.297	0.391±0.047
[NeIII]	3868	0.265±0.012	0.521±0.098	–	0.234±0.027
HeI+H_8	3887	0.126±0.007	–	–	0.106±0.014
[NeIII]+H_ε	3968	0.153±0.008	–	0.203±0.039	0.163±0.018
H_δ	4102	0.154±0.008	–	0.253±0.043	0.238±0.023
H_γ	4340	0.474±0.017	0.380±0.069	0.470±0.058	0.470±0.033
[OIII]	4363	0.160±0.008	–	–	0.136±0.012
H_β	4861	1.000	1.000	1.000	1.000
[OIII]	4959	1.685±0.044	1.286±0.122	1.000±0.057	1.743±0.053
[OIII]	5007	4.570±0.100	3.950±0.315	2.852±0.148	4.975±0.140
H_α	6563	–	2.859±0.551	–	–
$c(H_\beta)$		0.000±0.115	0.198±0.125	0.471±0.198	0.097±0.113
$EW(H_\beta)$		137	32	56	115
d, Mpc		19	113	94	153
M_B		-13.39	-18.27	-16.87	-18.42
$L(H_\beta)$, erg·s^{-1}		$1.16\cdot10^{39}$	$1.31\cdot10^{40}$	$1.11\cdot10^{40}$	$8.63\cdot10^{40}$
T_e, K		19580±850	10370±880	9390±780	17640±1100
O^+/H^+ (*10^{-5})		0.189±0.036	6.430±4.077	7.884±5.205	0.214±0.076
O^{2+}/H^+ (*10^{-5})		2.923±0.449	12.63±5.75	12.89±5.641	3.718±0.776
Ne^{2+}/H^+ (*10^{-6})		3.262±0.629	43.92±27.38	–	3.701±1.258
12+log(O/H)		7.49±0.07	8.28±0.22	8.32±0.23	7.60±0.09
12+log(Ne/H)		6.55±0.08	7.87±0.27	–	6.60±0.15

Table 3—(*continued*)

Line	λ_0	Galaxy			
		1305+547	1307+563	1319+579B	1319+579A
[OII]	3727	2.349±0.442	1.261±0.272	1.668±0.244	0.471±0.036
H_{11}	3766	–	–	–	0.025±0.003
H_{10}	3793	–	–	–	0.034±0.004
H_9	3832	–	–	–	0.043±0.005
[NeIII]	3868	0.281±0.058	0.456±0.097	0.287±0.045	0.386±0.026
HeI+H_8	3887	0.192±0.041	0.203±0.047	0.143±0.025	0.129±0.011
[NeIII]+H_ϵ	3968	0.218±0.042	0.209±0.045	0.191±0.030	0.262±0.018
H_δ	4102	0.208±0.036	0.286±0.053	0.286±0.037	0.263±0.016
H_γ	4340	0.470±0.058	0.470±0.064	0.470±0.044	0.470±0.021
[OIII]	4363	–	0.100±0.018	0.053±0.008	0.115±0.007
HeI	4471	–	–	–	0.040±0.003
[ArIV]+HeI	4712	–	–	–	0.045±0.002
[ArIV]	4740	–	–	–	0.020±0.001
H_β	4861	1.000	1.000	1.000	1.000
[OIII]	4959	1.494±0.076	1.850±0.102	1.300±0.052	2.510±0.044
[OIII]	5007	4.333±0.207	4.938±0.259	3.718±0.140	7.387±0.137
$c(H_\beta)$		0.770±0.200	0.796±0.219	0.831±0.151	0.471±0.071
$EW(H_\beta)$		112	65	75	293
d,Mpc		195	103	46	41
M_B		−20.95	−17.07	−14.81	−14.58
$L(H_\beta)$, erg·s^{-1}		$7.30\cdot 10^{41}$	$2.02\cdot 10^{40}$	$2.60\cdot 10^{39}$	$9.48\cdot 10^{39}$
T_e, K		10820±930	15080±1610	13090±980	13810±460
$O^+/H^+ (*10^{-5})$		6.543±4.132	1.084±0.708	2.259±1.096	0.534±0.086
$O^{2+}/H^+ (*10^{-5})$		12.33±5.113	5.490±2.318	5.796±1.861	9.598±1.338
$Ne^{2+}/H^+ (*10^{-5})$		2.014±1.277	1.090±0.694	1.059±0.513	1.203±0.249
$Ar^{3+}/H^+ (*10^{-7})$		–	–	–	3.496±0.611
He^+/H^+		–	–	–	0.085±0.007
12+log(O/H)		8.28±0.11	7.82±0.20	7.91±0.16	8.01±0.06
12+log(Ne/H)		7.54±0.28	7.13±0.28	7.20±0.21	7.11±0.09
12+log(Ar/H)		–	–	–	5.54±0.08
12+log(He/H)		–	–	–	10.93±0.04

Table 3—(*continued*)

Line	λ_o	Galaxy			
		Mkn 1481	1342+562A	1342+562B	Mkn 1486
[OII]	3727	1.522±0.034	2.225±0.156	4.574±1.225	1.224±0.039
[NeIII]	3868	0.622±0.018	0.415±0.027	0.702±0.185	0.405±0.017
HeI+H_8	3887	0.249±0.011	0.183±0.013	–	0.084±0.006
[NeIII]+H_ε	3968	0.299±0.012	0.305±0.019	–	0.200±0.011
H_δ	4102	0.239±0.011	0.270±0.018	–	0.286±0.014
H_γ	4340	0.482±0.018	0.463±0.016	0.769±0.129	0.485±0.020
[OIII]	4363	0.049±0.005	0.084±0.006	–	0.119±0.008
HeI	4471	–	0.056±0.004	–	0.048±0.004
H_β	4861	1.000	1.000	1.000	1.000
[OIII]	4959	1.597±0.053	1.591±0.035	0.539±0.072	1.415±0.084
[OIII]	5007	4.405±0.130	4.744±0.096	2.937±0.266	3.908±0.165
HeI	5876	–	–	–	0.097±0.009
H_α	6563	–	–	–	2.850±0.108
[NII]	6584	–	–	–	0.217±0.023
$c(H_\beta)$		0.900±0.025	0.000±0.092	0.000±0.350	0.000±0.133
$EW(H_\beta)$		56	143	40	69
d, Mpc		37	424	423	203
M_B		−15.84	−21.14	−20.13	−19.98
$L(H_\beta)$, erg·s^{-1}		$5.08 \cdot 10^{39}$	$7.94 \cdot 10^{41}$	$7.37 \cdot 10^{40}$	$1.51 \cdot 10^{41}$
T_e, K		10700±460	14540±590	10760±280	18630±1200
$O^+/H^+ (*10^{-5})$		4.431±1.084	2.146±0.515	12.99±5.257	0.583±0.154
$O^{2+}/H^+ (*10^{-5})$		13.14±2.810	5.616±0.894	7.468±1.568	2.622±0.644
$Ne^{2+}/H^+ (*10^{-6})$		46.53±11.32	11.07±2.493	51.26±20.27	5.605±1.499
$N^+/H^+ (*10^{-6})$		–	–	–	1.120±0.314
He^+/H^+			0.119±0.009	–	–
12+log(O/H)		8.24±0.10	7.89±0.07	8.31±0.14	7.51±0.06
12+log(Ne/H)		7.79±0.11	7.18±0.10	8.15±0.17	6.96±0.17
12+log(N/H)		–	–	–	6.79±0.20
12+log(He/H)		–	11.11±0.03	–	10.98±0.05

Table 3—(*continued*)

Line	λ_o	Galaxy			
		1408+551A	1408+551B	1423+518	1430+521
[OII]	3727	–	0.764±0.057	1.215±0.162	1.446±0.225
H_{12}	3749	–	0.054±0.005	–	–
H_{10}	3793	–	0.077±0.007	–	–
H_9	3832	–	–	0.207±0.065	–
[NeIII]	3868	–	0.445±0.030	0.222±0.070	0.332±0.053
HeI+H_8	3887	–	0.181±0.013	0.210±0.065	0.150±0.026
[NeIII]+H_ε	3968	–	0.251±0.016	0.187±0.061	0.151±0.025
HeI	4026	–	0.058±0.005	–	–
H_δ	4102	–	0.242±0.014	0.375±0.096	0.236±0.036
H_γ	4340	–	0.490±0.021	0.478±0.109	0.470±0.047
[OIII]	4363	–	0.081±0.006	–	0.079±0.012
HeI	4471	–	0.044±0.004	–	–
HeII	4686	–	0.122±0.007	–	–
H_β	4861	–	1.000	1.000	1.000
HeI	4921	–	0.031±0.003	–	–
[OIII]	4959	–	2.005±0.044	1.495±0.259	1.721±0.074
[OIII]	5007	–	5.243±0.107	4.212±0.622	4.726±0.190
$c(H_\beta)$		–	0.000±0.096	0.000±0.175	0.370±0.161
$EW(H_\beta)$		–	147	83	81
d, Mpc		244	466	43	154
M_B		−19.44	−20.84	−14.37	−18.44
$L(H_\beta)$, $erg \cdot s^{-1}$		–	$9.05 \cdot 10^{41}$	$2.46 \cdot 10^{39}$	$5.30 \cdot 10^{40}$
T_e, K		–	13490±520	10240±110	13820±1120
$O^+/H^+ (*10^{-5})$		–	0.949±0.233	4.224±0.810	1.636±0.830
$O^{2+}/H^+ (*10^{-5})$		–	7.748±1.272	14.32±2.900	6.567±2.203
$Ne^{2+}/H^+ (*10^{-6})$		–	14.92±3.478	19.63±7.301	10.32±5.155
He^+/H^+		–	0.094±0.009	–	–
12+log(O/H)		–	7.94±0.08	8.27±0.09	7.91±0.16
12+log(Ne/H)		–	7.22±0.10	7.40±0.16	7.13±0.22
12+log(He/H)		–	10.98±0.04	–	–

Table 3—(*continued*)

Line	λ_o	Galaxy			
		1432+530	1523+589	Mkn 483	1533+574B
[OII]	3727	2.942±0.253	3.657±1.233	3.844±0.984	0.662±0.100
[NeIII]	3868	0.601±0.063	0.571±0.201	–	0.306±0.044
HeI+H_8	3887	0.201±0.026	–	–	0.055±0.011
[NeIII]+H_ε	3968	0.188±0.021	0.371±0.125	–	–
H_δ	4102	0.257±0.023	–	–	0.230±0.029
H_γ	4340	0.504±0.023	0.463±0.107	–	0.470±0.043
[OIII]	4363	–	–	–	0.105±0.012
H_β	4861	1.000	1.000	1.000	1.000
[OIII]	4959	1.282±0.046	1.347±0.126	1.036±0.163	1.560±0.062
[OIII]	5007	3.427±0.103	4.409±0.378	1.963±0.279	4.368±0.166
[OI]	6300	–	0.465±0.147	–	–
[OI]	6363	–	0.359±0.122	–	–
HeI	5876	–	–	–	0.137±0.019
H_α	6563	–	–	2.859±0.758	2.153±0.309
[NII]	6584	–	–	–	0.066±0.013
HeI		–	–	–	0.075±0.015
[SII]	6717	–	–	–	0.148±0.028
[SII]	6731	–	–	–	0.118±0.023
$c(H_\beta)$		0.000±0.113	1.396±0.357	0.901±0.172	0.249±0.148
$EW(H_\beta)$		36	58	4	89
d,Mpc		270	357	290	68
M_B		−19.66	−20.77	−20.32	−17.15
$L(H_\beta)$, erg·s^{-1}		$5.90\cdot10^{40}$	$2.47\cdot10^{41}$	$1.31\cdot10^{40}$	$2.18\cdot10^{40}$
T_e, K		10590±130	11300±990	10220±870	16460±1260
$O^+/H^+(*10^{-5})$		7.405±1.101	8.529±6.216	13.47±9.57	0.445±0.199
$O^{2+}/H^+(*10^{-5})$		10.64±0.886	10.66±4.310	13.12±6.83	4.034±1.169
$Ne^{2+}/H^+(*10^{-6})$		46.73±7.721	34.77±25.32	–	5.781±2.492
$N^+/H^+(*10^{-7})$		–	–	–	4.256±1.771
$S^+/H^+(*10^{-7})$		–	–	–	1.098±0.446
12+log(O/H)		8.26±0.05	8.28±0.24	8.45±0.06	7.65±0.13
12+log(Ne/H)		7.90±0.07	7.87±0.32	–	6.82±0.19
12+log(N/H)		–	–	–	6.63±0.18
12+log(S/H)		–	–	–	6.04±0.18

Table 3—(continued)

Line	λ_o	Galaxy			
		0756+611	0805+607	1001+555	1524+575A
[OII]	3727	3.576±0.540	1.791±0.214	2.198±0.478	2.936±0.503
H_γ	4340	–	0.612±0.095	0.486±0.089	0.566±0.096
H_β	4861	1.000	1.000	1.000	1.000
[OIII]	4959	1.050±0.109	0.617±0.096	1.387±0.152	0.610±0.077
[OIII]	5007	2.364±0.211	1.855±0.219	4.236±0.384	1.026±0.115
H_α	6563	2.859±0.444	–	2.859±0.672	2.859±0.424
[NII]	6584	0.447±0.089	–	–	–
[SII]	6717	0.741±0.141	–	–	–
[SII]	6731	0.654±0.126	–	–	–
$c(H_\beta)$		0.170±0.101	0.000±0.499	0.286±0.152	1.167±0.096
$EW(H_\beta)$		8	15	165	12
d, Mpc		123	188	24	182
M_B		−17.96	−19.38	−13.86	−19.30
$L(H_\beta)$, erg·s^{-1}		$3.27 \cdot 10^{39}$	$2.98 \cdot 10^{40}$	$6.44 \cdot 10^{38}$	$8.15 \cdot 10^{39}$
T_e, K		10280±870	8570±6840	10660±920	8810±710
$O^+/H^+(*10^{-5})$		12.26±7.410	13.89±8.423	6.441±4.275	20.24±13.19
$O^{2+}/H^+(*10^{-5})$		8.480±3.957	5.326±2.790	12.35±5.720	7.038±3.592
$N^+/H^+(10^{-6})$		8.021±4.125	–	–	–
$S^+/H^+(10^{-6})$		2.744±1.390	–	–	–
12+log(O/H)		8.32±0.24	8.28±0.20	8.27±0.23	8.44±0.27
12+log(N/H)		7.13±0.22	–	–	–
12+log(S/H)		6.67±0.22	–	–	–

Table 3—(*continued*)

Line	λ_o	Galaxy			
		0745+587	0751+570	1118+578B	1526+585B
[OII]	3727	2.166±0.501	1.369±0.095	1.191±0.160	4.023±0.775
H_γ	4340	–	0.485±0.047	–	–
H_β	4861	1.000	1.000	1.000	1.000
[OIII]	4959	1.167±0.174	0.230±0.028	1.804±0.182	1.041±0.119
[OIII]	5007	2.839±0.364	0.931±0.071	4.716±0.432	3.785±0.363
H_α	6563	2.859±0.675	–	2.819±0.354	2.859±0.669
$c(H_\beta)$		0.020±0.154	0.000±0.312	0.000±0.163	0.498±0.152
$EW(H_\beta)$		14	15	5	5
d, Mpc		127	160	44	182
M_B		−17.52	−19.41	−16.70	−18.98
$L(H_\beta)$, $erg \cdot s^{-1}$		$2.24 \cdot 10^{39}$	$2.75 \cdot 10^{40}$	$3.35 \cdot 10^{38}$	$5.52 \cdot 10^{39}$
T_e, K		9820±820	6770±485	10610±910	11090±960
$O^+/H^+(*10^{-4})$		0.880±0.614	3.916±2.328	0.316±0.210	1.017±0.642
$O^{2+}/H^+(*10^{-4})$		1.154±0.736	1.549±0.786	1.461±0.676	0.947±0.438
12+log(O/H)		8.31±0.29	8.75±0.06	8.26±0.21	8.29±0.24

Line	λ_o	Galaxy			
		1149+579	1212+563	1305+542	1457+540
[OII]	3727	1.368±0.444	0.940±0.397	1.605±0.479	0.327±0.082
H_γ	4340	0.470±0.098	0.470±0.123	0.470±0.093	0.816±0.111
H_β	4861	1.000	1.000	1.000	1.000
[OIII]	4959	0.664±0.071	2.372±0.245	0.603±0.061	0.554±0.063
[OIII]	5007	1.493±0.146	6.605±0.659	1.757±0.154	2.316±0.195
$c(H_\beta)$		0.286±0.338	0.551±0.422	0.551±0.317	0.000±0.292
$EW(H_\beta)$		29	54	34	12
d, Mpc		190	290	180	160
M_B		−18.92	−17.81	−19.26	−18.52
$L(H_\beta)$, $erg \cdot s^{-1}$		$3.48 \cdot 10^{40}$	$1.79 \cdot 10^{40}$	$6.05 \cdot 10^{40}$	$1.42 \cdot 10^{40}$
T_e, K		7910±610	11480±1010	8320±660	7577±270
$O^+/H^+(*10^{-4})$		1.586±1.309	0.208±0.178	1.441±1.138	0.485±0.238
$O^{2+}/H^+(*10^{-4})$		1.366±0.692	1.589±0.729	1.228±0.603	2.171±0.616
12+log(O/H)		8.47±0.29	8.25±0.22	8.43±0.28	8.42±0.14

Table 3—(*continued*)

Line	λ_o	Galaxy			
		0926+607	1047+598	1114+587	1520+572
[OII]	3727	2.441±0.281	1.512±0.173	3.087±0.233	2.135±0.216
H_β	4861	1.000	1.000	1.000	1.000
[OIII]	4959	1.421±0.183	2.778±0.280	1.661±0.141	0.117±0.028
[OIII]	5007	4.337±0.450	6.321±0.557	5.057±0.353	0.646±0.087
$c(H_\beta)$		–	–	–	–
$EW(H_\beta)$		12	11	7	17
d,Mpc		84	512	34	433
M_B		−16.62	−20.45	−15.14	−21.18
$L(H_\beta)$, $erg \cdot s^{-1}$		$1.56 \cdot 10^{39}$	$9.00 \cdot 10^{40}$	$2.81 \cdot 10^{38}$	$1.15 \cdot 10^{41}$
T_e, K		10820±930	11710±1030	11440±1000	7240±540
$O^+/H^+ (*10^{-5})$		6.777±3.785	3.103±1.685	6.921±4.607	40.26±24.81
$O^{2+}/H^+ (*10^{-5})$		12.15±5.780	15.19±6.797	12.01±5.188	7.177±4.064
12+log(O/H)		8.28±0.22	8.26±0.20	8.28±0.22	8.68±0.26

Line	λ_o	Galaxy			
		1011+600B	1122+575	1522+588	1524+575B
[OII]	3727	4.101±0.927	4.127±0.563	0.181±0.081	1.418±0.193
H_β	4861	1.000	1.000	1.000	1.000
[OIII]	4959	1.742±0.201	0.646±0.048	1.175±0.210	0.736±0.118
[OIII]	5007	4.742±0.471	2.508±0.158	2.211±0.355	2.077±0.261
H_α	6563	2.859±0.667	2.859±0.425	2.859±0.780	–
[NII]	6584	–	–	0.477±0.089	–
[SII]	6717	–	–	0.761±0.251	–
$c(H_\beta)$		0.805±0.151	0.256±0.096	0.264±0.177	–
$EW(H_\beta)$		13	21	21	8
d,Mpc		47	27	203	241
M_B		−15.85	−14.65	−19.54	−19.91
$L(H_\beta)$, $erg \cdot s^{-1}$		$8.38 \cdot 10^{38}$	$2.64 \cdot 10^{38}$	$5.43 \cdot 10^{40}$	$3.20 \cdot 10^{40}$
T_e, K		11706±1032	10420±890	7960±620	8540±680
$O^+/H^+ (*10^{-4})$		0.844±0.553	1.411±0.828	0.204±0.194	1.116±0.385
$O^{2+}/H^+ (*10^{-5})$		10.85±4.980	7.910±3.451	21.51±12.36	7.368±3.917
12+log(O/H)		8.29±0.24	8.34±0.23	8.37±0.26	8.27±0.18

Table 3—(*continued*)

Line	λ_o	Galaxy			
		0134+318	0158+336	1119+601	1147+520
[OII]	3727	1.021±0.153	1.084±0.144	–	0.908±0.070
H_β	4861	1.000	1.000	–	1.000
[OIII]	4959	–	–	–	1.704±0.114
[OIII]	5007	–	–	–	5.208±0.305
[NII]		–	0.453±0.077	–	–
H_α	6563	–	2.439±0.273	–	–
[NII]	6584	–	1.378±0.174	–	–
$c(H_\beta)$		–	0.000±0.135	–	–
$EW(H_\beta)$		9	5	–	22
d,Mpc		268	227	67	22
M_B		−19.14	−18.78	−16.60	−15.21
$L(H_\beta)$, $erg \cdot s^{-1}$		$1.91 \cdot 10^{40}$	$4.49 \cdot 10^{39}$	–	$1.15 \cdot 10^{39}$
T_e, K		–	–	–	10660±200
$O^+/H^+ (*10^{-4})$		–	–	–	0.268±0.046
$O^{2+}/H^+ (*10^{-4})$		–	–	–	1.528±0.213
12+log(O/H)		–	–	–	8.25±0.06

Line	λ_o	Galaxy			
		0335−057B	0943+561A	1124+580	Mkn 826
[OII]	3727	1.779±0.212	–	–	–
H_γ	4340	–	0.615±0.066	–	0.468±0.054
H_β	4861	1.000	1.000	1.000	1.000
[OIII]	4959	–	2.293±0.180	1.741±0.356	1.465±0.111
[OIII]	5007	–	5.495±0.370	2.796±0.512	3.388±0.265
$c(H_\beta)$		–	0.000±0.321	–	0.930±0.364
$EW(H_\beta)$		7	98	8	11
d,Mpc		547	179	116	17
M_B		**−21.42**	−17.27	−17.83	−15.50
$L(H_\beta)$, $erg \cdot s^{-1}$		$1.18 \cdot 10^{41}$	$1.49 \cdot 10^{40}$	$2.45 \cdot 10^{39}$	$9.59 \cdot 10^{38}$
T_e, K		–	10650±910	–	9020±730
$O^+/H^+ (*10^{-5})$		–	–	–	–
$O^{2+}/H^+ (*10^{-5})$		–	17.29±7.58	–	18.76±8.770
12+log(O/H)		–	8.24±0.19	–	8.27±0.20

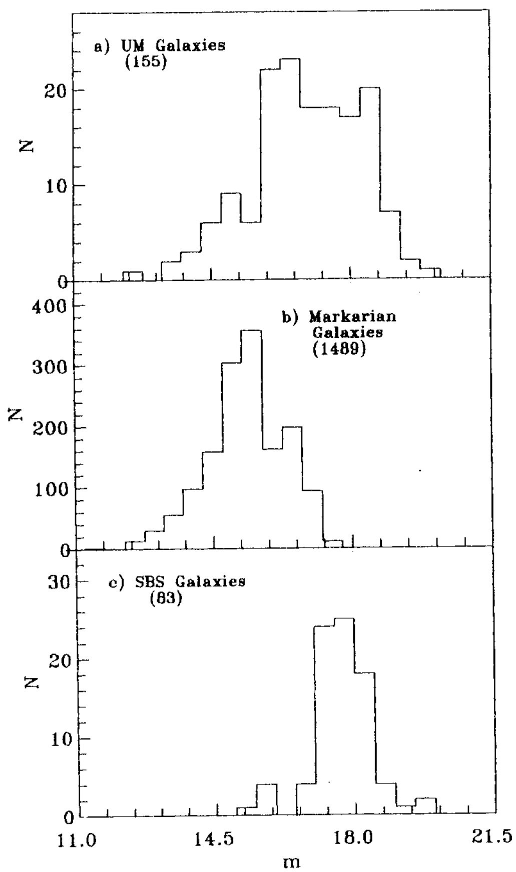

Figure 2 Apparent magnitude distributions for (a) the UM galaxies (Salzer *et al.*, 1989), (b) the Markarian galaxies (Mazzarella and Balzano, 1986) and (c) SBS galaxies.

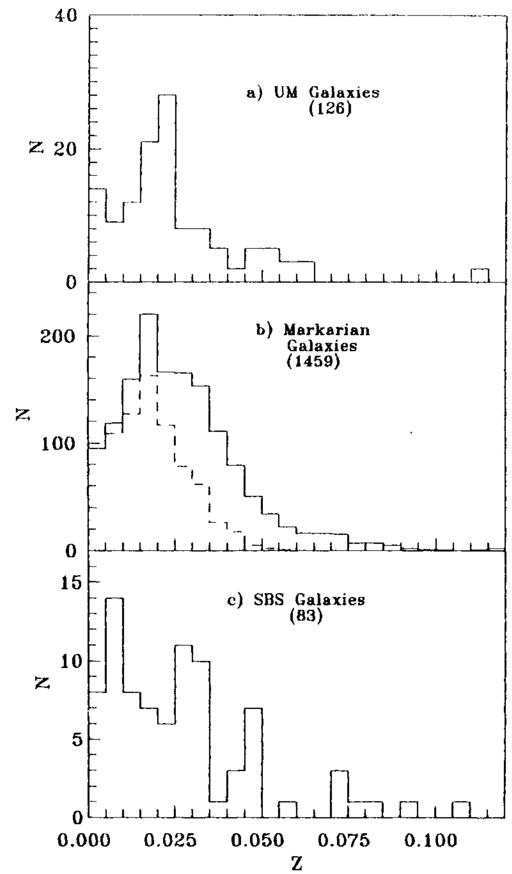

Figure 3 Redshift distributions for (a) UM galaxies (Salzer *et al.*, 1989) (b) Markarian galaxies (the solid line is a fit to all of the data, the dashed line is fit for the galaxies with $M_V > -20$) (Markarian *et al.*, 1989) and (c) the blue compact dwarf galaxies from SBS.

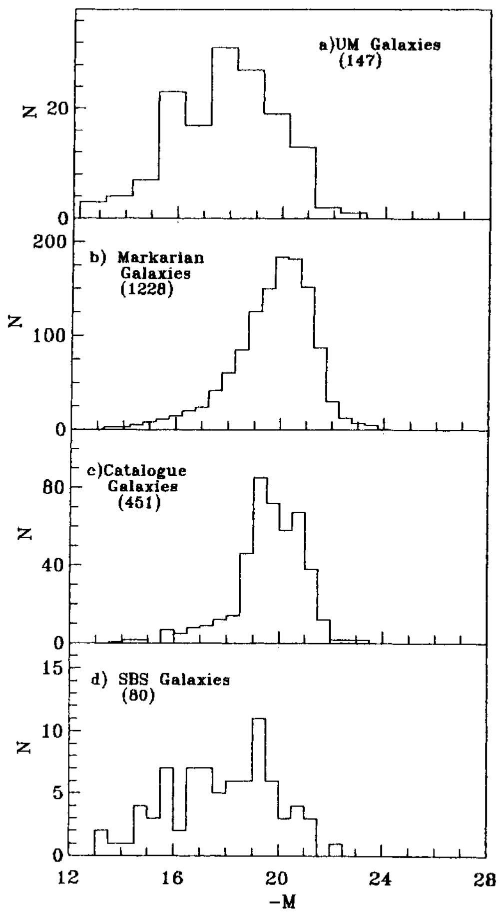

Figure 4 Absolute magnitude distributions for (a) the UM emission line galaxies (Salzer *et al.*, 1989), (b) the Markarian UV-excess galaxies (Mazzarella and Balzano, 1986), (c) the normal galaxies from the Catalogue sample (Nilson, 1973, Zwicky *et al.*, 1961–1968) and (d) BCDGs from SBS.

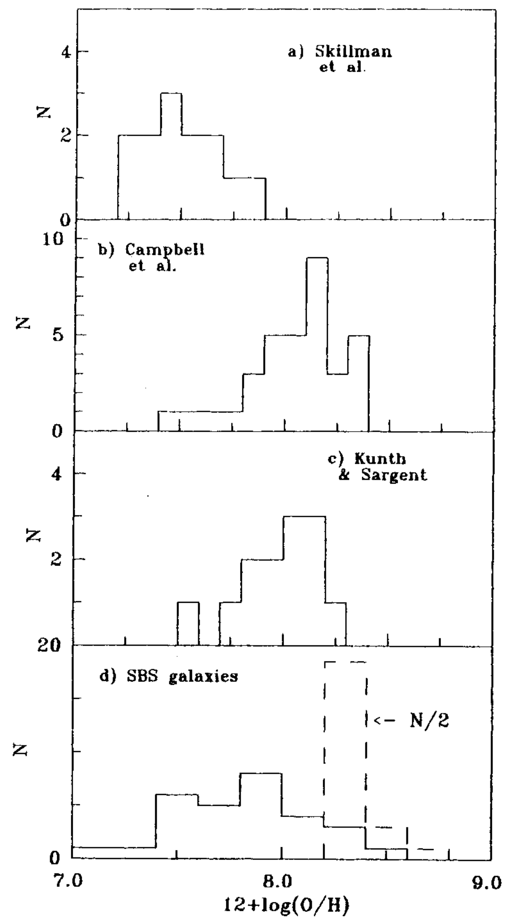

Figure 5 Oxygen abundance distribution of galaxies from the spectroscopic survey (a) (Skillman *et al.*, 1989) (b) (Campbell *et al.*, 1986), (c) Kunth and Sargent, 1983) and (d) present paper.

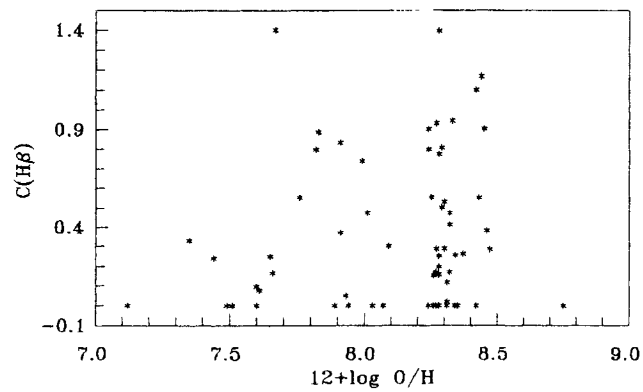

Figure 6 Extinction coefficient c (H_β) plotted vs heavy element abundance.

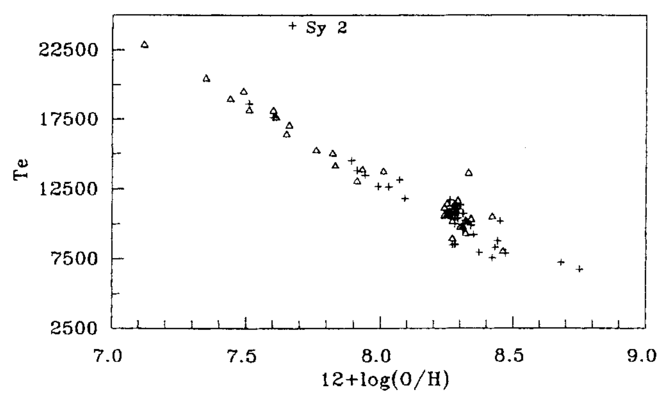

Figure 7 Electron temperature T_e as a function of heavy element abundance. Crosses denote galaxies with $M_v < -18^m$, triangles denotes galaxies with $M_v > -18^m$.

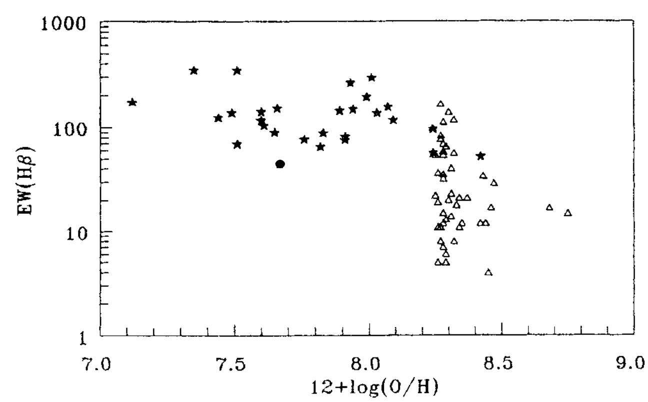

Figure 8 The H_β line equivalent widths plotted vs heavy element abundance. The galaxies, for which T_e were obtained by [OIII] 4959 + 5007/4363 ratios, are marked with stars.

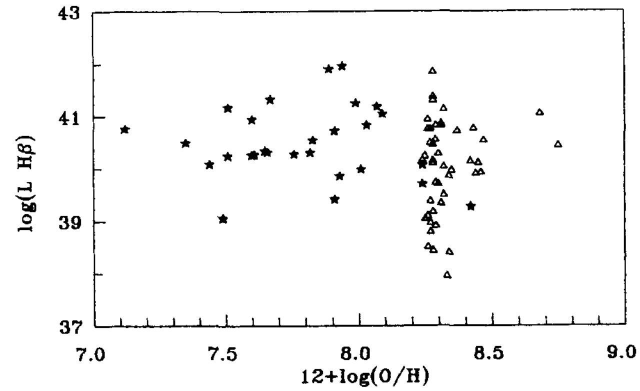

Figure 9 Logarithm of the H_β absolute luminosities against heavy element abundance. Symbols are the same as in Figure 8.

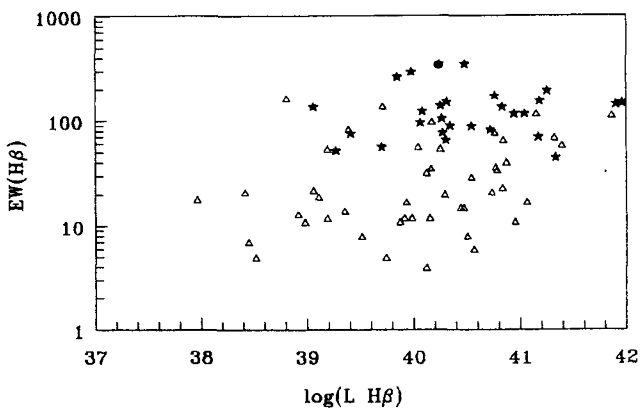

Figure 10 The H_β line equivalent widths plotted vs logarithm of the H_β-absolute luminosities. Designations are the same as in Figure 8.

References

Afanasiev, V. L., Lipovetsky, V. A., Michailov, V. P., Nazarov, E. A. and Shapovalova, A. I. (1991). The spectra reduction on the BTA scanner. *Astrofizitsheskie issledovanija* **31**, 121–133.

Aller, L. H. (1984). *Physics of Thermal Gaseous Nebulae*. Dordrecht, Reidel.

Bingelli, B., Sandage, A. and Tammann, G. A. (1985). Studies of the Virgo cluster area. *Astron. J.* **90,** 1681–1758.

Bohuski, T. J., Fairall, A. P. and Weedman, D. W. (1978) The nature of Tololo emission-line galaxies. *Astrophys. J.* **221,** 776–787.

Campbell, A., Terlevich, R. and Melnick, J. (1986). The stellar populations and evolution of HII galaxies—I. High signal-to-noise optical spectroscopy. *Mon. Not. RAS* **223,** No. 4, 811–826.

French, H. B. (1981). The ionization structure and abundance of argon in gaseous nebulae. *Astrophys. J.* **246,** No. 2, 434–443.

Gonzales-Riestra, R., Rego, M. and Zamorano, J. (1988). Star-forming knots in Mkn 178. *Astron. Astrophys.* **202,** No. 1/2, 27–34.

Izotov, Yu. I. (1990). On the role of molecular hydrogen in formation and evolution of blue compact dwarf galaxies and giant HII-regions. In *Physical Processes in Fragmentation and Star Formation.*: Kluwer Academic Publishers, 35–47.

Izotov, Yu. I., Lipovetsky, V. A., Guseva, N. G., Kniazev, A. Yu. and Stepanian, J. A. (1990). Unusually low heavy-element abundance found in the blue compact dwarf galaxy SBS 0335-052. *Nature* **343,** 238–238.

Kunth, D., Sargent, W. L. W. and Kowal, C. (1981). A spectroscopic survey of emission-line objects in two fields. *Astron. Astrophys.* **44,** 229–239.

Kunth, D. and Sargent, W. L. W. (1983). Spectrophotometry of 12 metal-poor galaxies: implications for the primordial helium abundance. *Astrophys. J.* **273,** 81–98.

Kunth, D., Maurogordato, S. and Vigroux, L. (1988). CCD observations of blue compact galaxies: a mixed bag of morphological types. *Astron. Astrophys.* **204,** No. 1/2, 10–20.

Lequeux, J., Peimbert, M., Rego, J. F., Serrano, A. and Torres-Peimbert, S. (1979). Chemical composition and evolution of irregular and blue compact galaxies. *Astron. Astrophys.* **80,** No. 2, 155–166.

Markarian, B. E., Lipovetsky, V. A. and Stepanian, J. A. (1983). Second Byurakan spectral sky survey. I. Quasistellar and Seyfert objects. *Astrofizika* **19,** No. 2, 29–43.

Markarian, B. E., Lipovetsky, V. A., Stepanian, J. A., Erastova, L. K. and Shapovalova, A. I. (1989). The First Byurakan survey. A catalogue of galaxies with UV-continuum. *Communications of the Special Astrophysical Observatory,* **62,** 5–117.

Mazzarella, J. M. and Balzano, V. A. (1986). A catalog of Markarian galaxies. *Astrophys. J. Suppl. Ser.,* **62,** No. 4, 751–820.

McCall, M. L., Rybski, P. M. and Shilds, G. A. (1985). The chemistry of galaxies. I. The nature of giant extragalactic HII regions. *Astrophys. J. Suppl. Ser.* **57,** No. 1, 1–62.

Neizvestny, S. I. (1983). Atmospheric extinction in SAO AS USSR. *Astrofizitsheskie issledovanija* **17,** 26–39.

Neizvestny, S. I. (1987). A study of optical variability of the Seyfert 2 galaxy nuclei. I. *Astrofizitsheskie issledovanija* **24,** 3–26.

Nilson, P. (1973). Uppsala general catalogue of galaxies (Uppsala: *Royal Society of Sciences of Uppsala*) (UGC).

Pagel, B. E. J., Edmunds, M. G., Blackwell, D. E., Chun, M. S. and Smith, G. (1979). On the composition of HII regions in southern galaxies—I. NGC 300 and 1365. *Mon. Not. RAS* **189,** No. 1, 95–113.

Perrinotto, M. (1983). Optical and IR emission lines. In *Diffuse matter in galaxies*: Dordrecht, Reidel, 205–237.

Salzer, J. J., MacAlphine, G. M. and Boroson, T. A. (1989). Observations of a complete sample of emission-line galaxies. I. CCD imaging and spectroscopy of galaxies in UM lists IV and V. *Astrophys. J. Suppl. Ser.* **70,** 447–477.

Salzer, J. J., MacAlphine, G. M. and Boroson, T. A. (1989). Observations of a complete sample of emission-line galaxies. II. Properties of the UM survey galaxies. *Astrophys. J. Suppl. Ser.* **70,** 479–496.

Searle, L. and Sargent, W. L. W. (1972). Inferences from the composition of two dwarf blue galaxies. *Astrophys. J.* **173,** No. 1, 25–34.

Skillman, E. D., Melnick, J., Terlevich, R. and Moles, M. (1988). The extremely low oxygen abundance of GR 8: a very low luminosity dwarf irregular galaxy. *Astron. Astrophys.* **196,** No. 1/2, 31–38.

Skillman, E. D., Kennicutt, R. C. and Hodge, P. W. (1989). Oxygen abundances in nearby dwarf irregular galaxies. *Astrophys. J.* **347,** No. 2, 875–882.

Smith, M. G., Aguirre, C. and Zemelman, M. (1976). Emission-line galaxies and quasars. II. The classification systems and list N1, declination $<-27.5°$, galactic latitude $>+20°$. *Astrophys. J. Suppl. Ser.* **32,** 217–231.

Takase, B. (1980). Counts of ultraviolet-bright galaxies and their distributions in clusters of galaxies. *Publ. Astron. Soc. Japan.* **32,** No. 4, 605–612.

Vikuljev, N. A., Zin'kovsky, V. V., Levitan, B. I., Nazarenko, A. F. and Neizvestny, S. I. (1991). Electrophotometer in the BTA Nasmyth-1 focus. *Astrofizitsheskie issledovanija* **33,** 158–175.

Whitford, A. E. (1958). The law of interstellar reddening, *Astron. J.* **63,** No. 5, 201–207.

Zwicky, F., Herzog, E., Wild, P. and Kowal, C. (1961–1968). Catalogue of galaxies and clusters of galaxies. (Pasadena: California Institute of Technology).

Zwicky, F. (1966). Compact galaxies and compact parts of galaxies. II. *Astrophys. J.* **143,** No. 1, 192–202.